UNIVERSITÀ DEGLI STUDI DI PADOVA

DIPARTIMENTO DI INGEGNERIA INDUSTRIALE

LAUREA MAGISTRALE IN INGEGNERIA CHIMICA E DEI PROCESSI INDUSTRIALI

Tesi di Laurea Magistrale in
Ingegneria Chimica e dei Processi Industriali

DESIGN AND SIMULATION OF HYDROGENATION PROCESSES FOR CO_2 CONVERSION TO C-1 CHEMICALS

Relatore: Prof. Fabrizio Bezzo

Correlatore: Dott.ssa Elena Barbera

Laureando: FABIO MANTOAN

ANNO ACCADEMICO 2018-2019

Abstract

The continuous rising of the global CO_2 emission and the alarming environmental effects that this involve are leading the researchers to develop new strategies in the field of the CO_2 reduction instead of the simple emission reduction. Among the different strategies proposed, the carbon capture and utilization (CCU) looks to be a very attractive option not only because it can reduce the CO_2 emissions but also because it can produce new chemicals from this waste material. The hydrogenation of CO_2 into five main chemicals: the methanol synthesis, the methane synthesis, the urea synthesis, the syngas synthesis and the formic acid synthesis, become therefore the study of this elaborate. Through the use of five technological parameters: the CO_2 conversion, the water production over the CO_2 treated in the process, the hydrogen requirement over the CO_2 treated in the process, the thermal energy consumption over the CO_2 treated in the process and the electricity consumption over CO_2 treated in the process, it is realize a comparison of these different synthesis in order to find the critical issues of the implementation of this unconventional processes for CO_2 reduction.

Riassunto

Con il crescente aumento delle emissioni di anidride carbonica e l'inevitabile riscaldamento globale che ciò comporta, l'umanità sta vivendo sulla propria pelle gli effetti anomali dovuti all'incuria e alla sottovalutazione nell'emettere senza troppo controllo questo gas in atmosfera. Attualmente, varie normative ed accordi internazionali sono in atto per il controllo e la riduzione di questo inquinante ma, per una sua efficace riduzione, si devono accoppiare a queste normative delle nuove strategie altamente tecnologiche che abbiano come fine un abbattimento intensivo e altamente efficiente della CO_2. Fra le varie tecniche attualmente disponibili, quella della cattura e dell'utilizzo della CO_2 come materia prima per la sintesi di nuovi composti sembra un'idea allettante, non solo perché questa permette di abbattere la CO_2, ma poiché permette di ottenere nuovi composti chimici da questo materiale inquinante e di scarto. Lo studio e la progettazione di questa soluzione tecnica diventa quindi lo scopo di questo elaborato. I processi studiati riguardano il processo di idrogenazione della CO_2 a cinque diversi composti chimici. Vengono quindi studiate ed approfondite le sintesi di: metanolo, metano, urea, gas di sintesi e acido formico. Lo scopo finale diviene allora quello di confrontare questi diversi processi mediante l'uso di cinque parametri tecnologici di riferimento: la conversione della CO_2, l'acqua prodotta per tonnellata di CO_2 trattata, il consumo di idrogeno per tonnellata di CO_2 trattata, il consumo di energia termica per tonnellata di CO_2 trattata ed infine, il consumo di elettricità per tonnellata di CO_2 trattata. I processi vengono inizialmente divisi in due famiglie: la prima, in cui vengono analizzati i processi che presentano uno studio scientifico accettato dalla comunità da cui vengono estratte le informazioni necessarie al confronto finale e la seconda, in cui attraverso pubblicazioni accademiche e brevetti internazionali, vengono progettati e simulati i processi per cui in letteratura scientifica non risultano ancora degli elaborati specifici. Una volta ricavati i parametri tecnologici di questi cinque processi, sono riassunti i risultati e le criticità riscontrate. Dal confronto finale fra i processi risulta che la sintesi della miscela di syngas è il processo con la più alta conversione, con un valore del 99.7%. Dal confronto della quantità di acqua prodotta dai processi, deriva che il processo del metano è quello che ne produce la più alta quantità, con un valore di 0.801 $tonH_2O/tonCO_2$, sprecando così l'idrogeno per ottenere un prodotto a valore industriale nullo mentre, il processo dell'acido formico non produce acqua. Dal confronto riguardante il consumo di idrogeno deriva una discreta regolarità fra i processi, con il processo del metanolo con il più basso consumo (0.136 $tonH_2/tonCO_2$). Dal confronto riguardante il consumo specifico di energia termica, deriva che il processo dell'urea, con un valore di 4.571 $MW_h/tonCO_2$ è il processo più dispendioso in termini energetici, considerando però che sono stati presi in considerazione i consumi per la sintesi dell'ammoniaca necessaria per lo svolgimento del processo. Dal confronto del consumo

specifico di energia elettrica è risultata ancora l'urea come il processo più dispendioso, con un valore di 0.955 $MW_h/tonCO_2$, per gli stessi motivi detti precedentemente.

Contents

Introduction

The growing world population and demand for energy has caused drastic increase of CO_2 emissions during the last two decades. Our society needs to face new challenges, such as mitigation of climate change, preservation of the environment, usage of renewable energy and replacement of fossil fuels. The realization of these challenges requires new breakthrough solutions in order to be successfully addressed. This thesis aims at investigating an unconventional process for the CO_2 abatement: the utilization of the CO_2 as a chemical feedstock. The process of CO_2 hydrogenation into value added C1 chemicals are thus investigated through four main chapters that discuss the context and the main promising processes that can be performed with this technology. The first chapter introduces the current scenario of CO_2 emissions and the related policy strategies to mitigate the climate change. After a focus on the general CO_2 separation technologies, the notions of carbon capture and utilisation (CCU) and the idea of using CO_2 as a chemical feedstock is then discussed, as well as the concept of using CO_2 as a platform for the production of new value added chemicals. The process of CO_2 hydrogenation is therefore briefly introduced and finally, the comparison metric between the processes are defined and discussed. The second chapter discusses singularly three different academic works that simulate the hydrogenation of CO_2: the methanol synthesis, the methane synthesis and the urea synthesis. This chapter, presents the state of art of processes that use CO_2 as a chemical feedstock, and for which simulation has already been carried out. The third chapter investigates the hydrogenation of the CO_2 to produce a syngas mixture. The study of this process and its simulation are built step by step according to the only, but detailed, patent found in literature. The reaction model, the thermodynamics and the relative assumptions are deeply discussed. The approach to the simulation and its implementation are then explained and discussed and, at the end, energy integration is applied to the process. The fourth chapter investigates the hydrogenation of the CO_2 to formic acid. First, the kinetic model and its parameters are estimated and optimized, and afterwards that, the thermodynamic approach used for the simulation and its assumptions are deeply discussed. Later, it is introduced the study of the reactor and its rigorous implementation in the process simulator. Finally, the simulation results are discussed. At the end, a conclusion summarizes the comparison of these different synthesis in order to find the critical issues of the implementation of this processes for the CO_2 reduction.

Chapter 1

Context and motivation for the Thesis

The first chapter introduces the current scenario of CO_2 emissions and the related policy strategies to mitigate the climate change, with a focus on the general CO_2 separation technologies and notions of carbon capture and utilisation (CCU). The idea of using CO_2 as a chemical feedstock is then discussed, as well as the concept of using CO_2 as a platform for the production of new value added chemicals. Later, the process of CO_2 hydrogenation is introduced, which will be discussed in depth, process by process, in the successive chapters. Finally, the aim of this thesis is discussed.

1.1 CO_2 emissions

The growing concerns about global climate change and the increasing social awareness towards environmental problems have created a need for more sustainable development. Thus, our society needs to face new challenges, such as mitigation of climate change, preservation of the environment, usage of renewable energy and replacement of fossil fuels. The realization of these challenges requires new breakthrough solutions in order to be successfully addressed. There is no doubt that carbon dioxide (CO_2) is a common factor in these great challenges (IPCC 2014). The increasing emissions of this greenhouse gas (GHG) are of large concern, and therefore nowadays a huge effort is dedicated to reduce emissions of GHG, especially carbon dioxide, which contributed in total to ca. 75% of 49 Gt CO_2eq (in 2010) GHG emissions (Figure 1 A). Carbon dioxide emissions have been constantly growing worldwide since the pre-industrial era, reaching the level of 35.9 Gt in 2014 (Le Quéré et al. 2015). This caused the increase of CO_2 concentration in the atmosphere from ca. 280 ppm (parts per million) in the mid-1800s to 397 ppm in 2014, with an average growth of 2 ppm/year in the last 10 years (IEA 2015). More than 60% of anthropogenic greenhouse gas emissions, over 90% of which are associated with CO_2, are coming from the energy sector. Between 1971 and 2013 an increase by 150% in global total primary energy supply (TPSE) has been observed, which is mainly caused by worldwide economic growth and development. Although for the last few decades a huge development of renewable and nuclear energy sources was observed (which are considered non-emitting energy sources), the world energy supply was relatively unchanged over the past 42 years, and fossil fuels still account for ca. 82% (in 2013) of the world primary energy supply (IEA 2015). Therefore, carbon dioxide emissions are strongly associated with the combustion of fossil fuels (Figure 1 B). Two fuels which accounted for the highest CO_2 emissions are coal and oil. Till the early 2000s, the shares of oil in global CO_2 emissions was exceeding those from coal. The situation changed at the beginning of 2000s, due to the higher consumption of coal by developing countries, such as India and China, where energy-intensive industrial processes are growing rapidly and large coal reserves are present. Power plants, petrochemical and chemical industry and cement industry are currently considered as the main sources of carbon dioxide emissions (Metz, B., Davidson, O., De Coninck, H., Loos, M., & Meyer 2005). However, electricity and heat generation accounted for 42% of global CO_2 emissions in 2013, making it the highest emitting sector (Figure 1 C). Such high emissions from energy and heat generation are associated with high consumption of coal, which has the highest carbon content per unit of energy released with respect to other fossil fuels. This trend is foreseen to be the same for the coming years, as many countries, such as Australia, China, India, Poland and South Africa produce over two thirds of electricity and heat from the combustion of fossil fuels (IEA 2015).

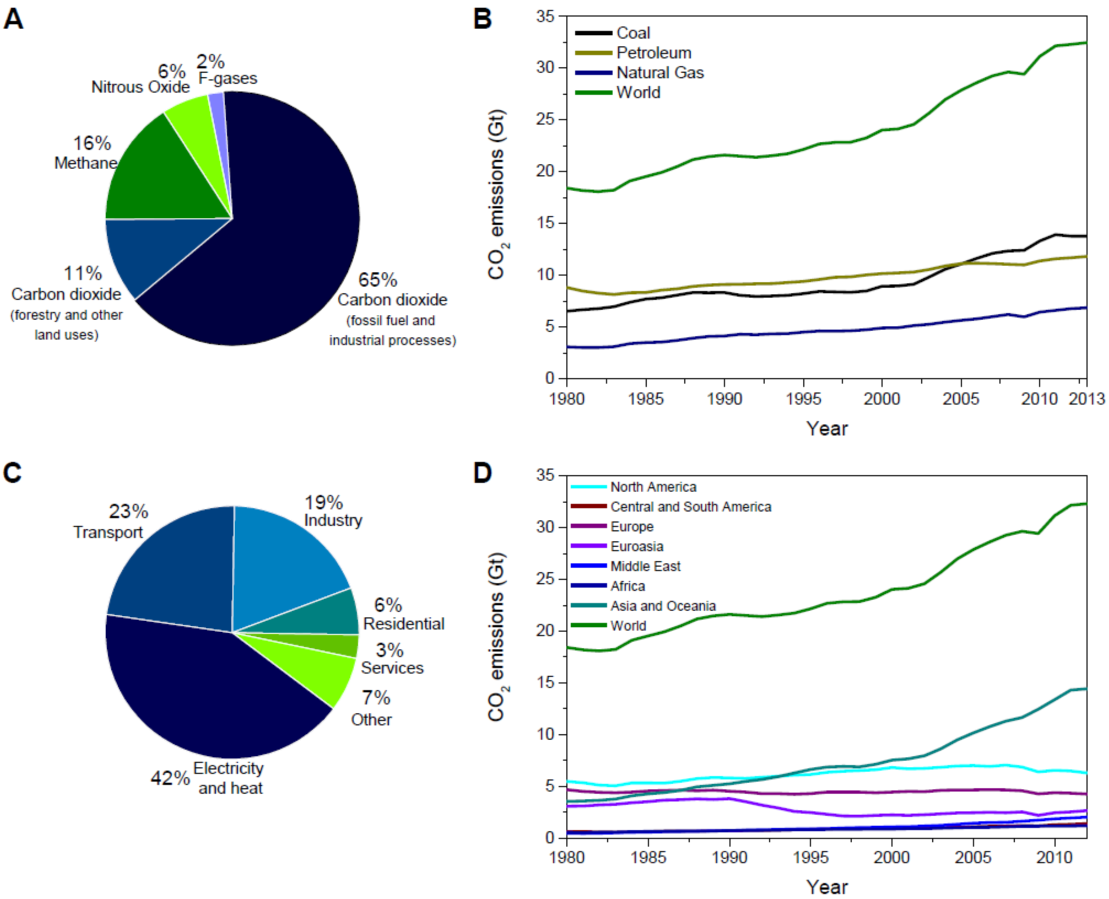

Figure 1 *The greenhouse gas emissions and CO_2 emissions: (A) global greenhouse gas emissions in 2010 by gas; (B) global CO_2 emissions by fuel in 1980-2013; (C) global CO_2 emissions by sector in 2013; global CO_2 emissions in 1980-2013 by region.*

The CO_2 emissions derived from energy production by country or region are dependent on the geopolitical situation, economy, type of fuel and energy mix. However, it is important to underline that top the 10 emitting countries (China, USA, India, Russia, Japan, Germany, Korea, Canada, Iran and Saudi Arabia) account for two thirds of global CO_2 emissions (IEA 2015). The region with the highest CO_2 emissions is Asia (mainly China and India) (Figure 1 D). In 2014, China increased its CO_2 emissions only by 0.9% with respect to 2013, which was the lowest annual increase observed in the last 10 years. The United States (second biggest emitter of CO_2) also showed increase of CO_2 emissions by 0.9% in 2014, which is lower than in the previous 2 years and was associated with a decrease in coal-fired power generation and increased consumption of natural gas. In 2014, the European Union continued to decrease emissions of CO_2 and due to the decrease in fossil-fuel consumption for power generation and lower demand for space heating, the EU-28 decreased the total CO_2 emissions by 5.4% (Olivier et al. 2013).

1.2 Reduction of CO_2 emissions – policies

It is important to understand global driving factors of CO_2 emissions in order to find effective solutions for reduction of greenhouse gases emissions. The growing world population and demand for energy has caused drastic increase of CO_2 emissions during last two decades. It is well known that the high increase of greenhouse gases emissions to the atmosphere in the last 150 years was caused mainly by well-developed countries, which emitted high amounts of GHG during industrial era (Figure 2).

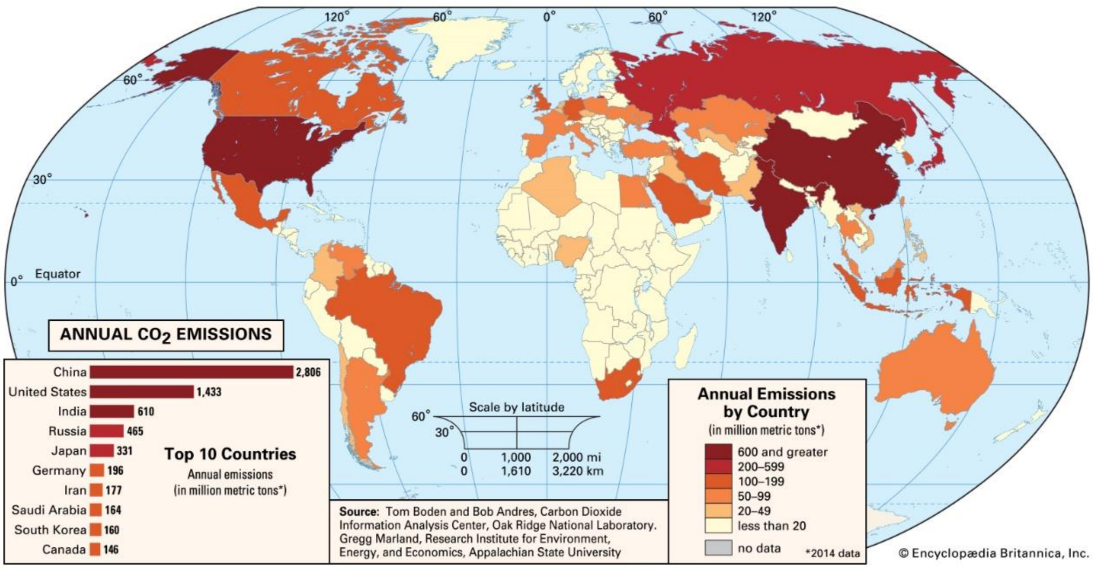

Figure 2 *Map of annual carbon dioxide emission by country in 2014.*

These countries in general apply today greenhouse gas emissions reduction policies, which are resulting in decreasing emissions. However, at the same time, currently developing countries emit enormous amounts of GHG. This is mainly caused by differences at economic, demographic and technological levels. Thus, in order for the world to develop in a sustainable way, the efforts must be undertaken by all countries. The first international agreement which forced reduction of GHG emissions was the Kyoto Protocol linked to the United Nations Framework Convention on Climate Change, adopted in 1997 and entered into force in 2005. In general, Kyoto Protocol stated that industrialised countries were required to reduce GHG emissions (CO_2, CH_4, N_2O, HFCs, PFCs, SF_6) on average by 5% against 1990 levels during the years 2008-2012 (first commitment period). The specific levels of reduction differed for each participating country depending on the political and economic situation (www.unfccc.int/kyoto_protocol). The second commitment period (years 2013-2020) requires to reduce GHG emissions by at least 18% with the respect to 1990 levels. In order to bring Kyoto's Protocol second commitment period into force, ratification by two-thirds of participating countries (144 countries) is required. Till 1st October 2015 only 49 countries have ratified Kyoto's Protocol second commitment period (IEA 2015). The fact that not all countries have ratified Kyoto Protocol, and some of the biggest emitters did not participate in it (United States), requires that new international agreements are established. In December 2015, in Paris, during COP21 (United Nations Conference on Climate Change) a new international climate agreement was finalised which will be applied from 2020. This agreement assumes the participation of both developed and developing countries. The goal is to limit global temperature increase to less than 2°C above industrial levels, which will be realised by reduction of GHG emissions (www.cop21.gouv.fr). European Union has been applying different GHG emission reduction policies for several years now, which resulted in the decrease of total CO_2 emissions by 0.4, 1.4 and 5.4%, respectively in 2012, 2013 and 2014 (Olivier et al. 2013). These achievements were reached thanks to the implementation of 20/20/20 policy which sets the following targets for year 2020 (Mignard and Pritchard 2008): (i) reduction of greenhouse gas emissions by 20%, (ii) the share of renewable energy at the level of at least 20%, and (iii) improvements in energy efficiency by 20%. In 2014 a new policy was accepted for the period of 2020-2030, which set new targets for 2030 year: (i) the reduction of GHG emissions by 40% with respect to 1990 level, (ii) at least 27% share of renewable energy consumption, and (iii) at least 27% energy saving compared with business-as-usual scenario (Pérez-Fortes, Bocin-Dumitriu, and Tzimas 2014). These policies frameworks are applied in order to develop low-carbon economy and meet EU long-term targets till 2050, which assume, among others, the reduction of GHG emissions by 80-95% as compared to 1900 levels (European Commission 2012).

1.3 Solutions for the reduction of CO_2 emissions

The generally accepted solutions for reducing CO_2 emissions into the atmosphere involve the implementation of three strategies (Hunt et al. 2010): (1) a reduction in energy consumption, (2) a change in what we consume, or (3) a change of our attitude towards resources and waste. Currently, the most developed strategies are (1) and (2). These two strategies are resulting in lower carbon consumption by the development of technologies with higher efficiency, the decrease in energy consumption per capita and the replacement of fossil fuel-based energy sources by renewable ones, such as wind, solar, biomass etc. However, there is a huge potential in changing our attitude towards greatly produced waste, including carbon dioxide. The implementation of carbon dioxide utilization processes is a key element to sustainable development, as strategies (1) and (2) have a limited capacity. Moreover, as it is predicted, fossil fuels will still be our main source of energy in the coming decades. The reduction of carbon dioxide can be realized either by carbon capture and storage (CCS) technologies or via utilization of carbon dioxide as a chemical feedstock – CCU (Carbon Capture and Utilization) as reported in Figure 3 (Hunt et al. 2010).

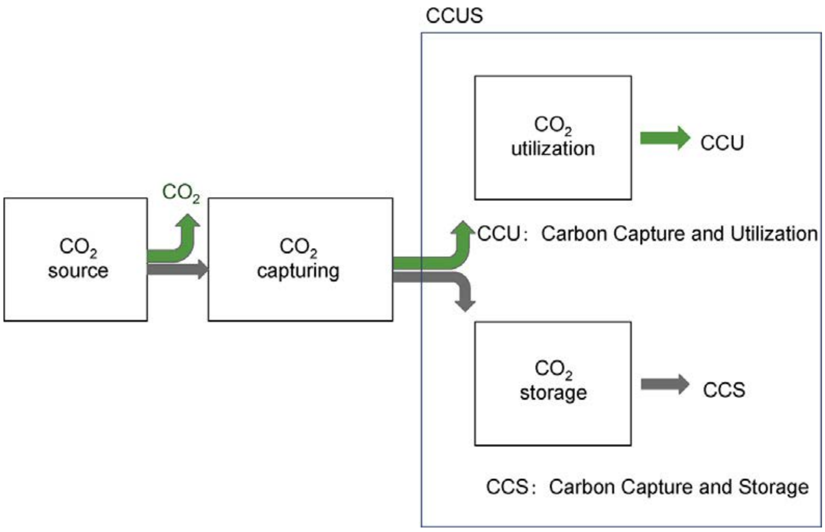

Figure 3: *The schematic representation of concept of carbon capture, utilization and storage (CCUS).*

These two approaches are complementary, and while CCS technologies are aiming at capturing and subsequently storing huge quantities of carbon dioxide, the chemical utilization of CO_2 aims at generating added-value products. It has to be noted that most technologies which are currently being developed as future CO_2 utilization processes, require pure streams of CO_2. Thus, the implementation of both solutions (CCS and chemical utilization of CO_2) is required.

1.4 Carbon capture and utilisation CCU

Carbon dioxide capture is already, or will be, applied to large scale stationary sources of emissions, such as fossil fuel power plants, fuel processing plants and other industrial installations (iron and steel, cement and bulk chemicals production). The capture of CO_2 from small and mobile sources (transportation, residential and commercial building sectors) would instead be rather difficult and more expensive than that from large stationary sources Therefore, currently capture systems from large scale sources are mainly developed. CO_2 capture systems from installations combusting fossil fuels and biomass include the following configurations (Figure 4) (Hunt et al. 2010): (i) post-combustion, (ii) precombustion, (iii) oxyfuel combustion, and (iv) capture from industrial process streams.

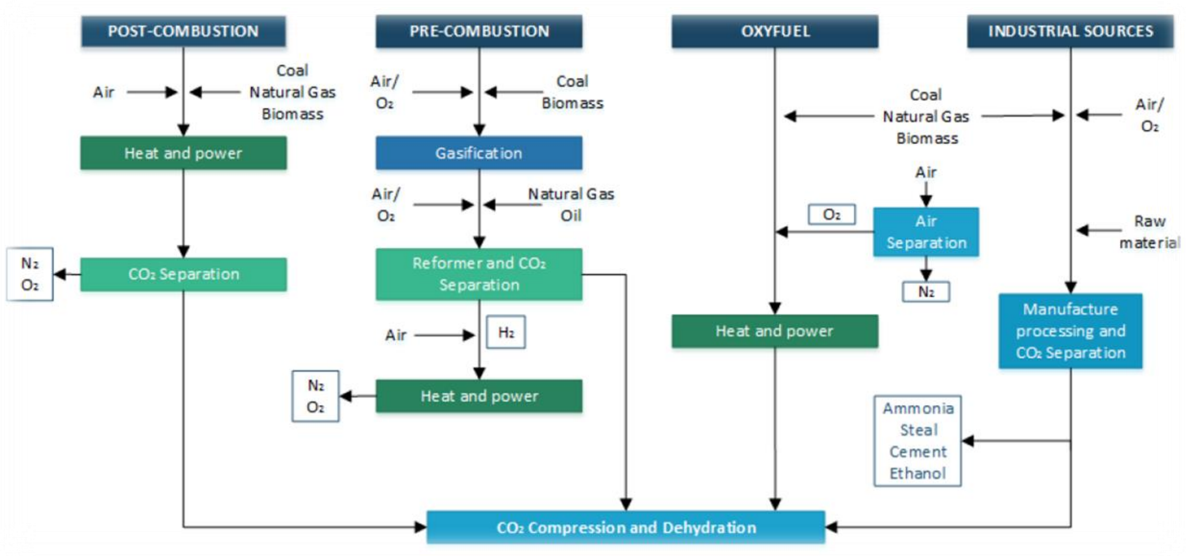

Figure 4: *Carbon dioxide capture systems from stationary sources*[12].

In the post-combustion capture systems, the fossil fuel or biomass is combusted in air. Flue gases are passed through a separation equipment which captures CO_2, and the remaining flue gas is discharged to the atmosphere. The post-combustion capture system can be applied in fossil fuel fired power plants. A pre-combustion capture system involves a reaction of a fuel in oxygen or air, and/or steam, in order to obtain synthesis gas (i.e. mixture of H_2 and CO) as the main product. The resulting carbon monoxide is further reacted with steam in the water gas shift reaction (WGS) to produce H_2 and CO_2 (Metz, B., Davidson, O., De Coninck, H., Loos, M., & Meyer 2005). CO_2 is subsequently separated. In this way a hydrogen-rich fuel is obtained which can be used in many applications, e.g. gas turbines, engines, fuel cells, boilers or furnaces. IGCC plants (Integrated Gasification Combined Cycle) use syngas as a fuel and can apply pre-combustion capture system. Oxyfuel combustion system assumes the combustion of fuel in a stream of pure oxygen instead of air. In this way, the produced flue gas consists mainly of CO_2 and H_2O. One of the drawbacks of this system is high flame temperatures, as a result of combustion of fuel in pure oxygen. However, a part of flue gases (H_2O and CO_2) can be recycled to the reactor in order to moderate combustion temperature. The second drawback is associated with high costs of oxygen separation from air. The capture of CO_2 from industrial processes can apply similar techniques as post-combustion, pre-combustion and oxyfuel combustion systems. This could be applied to processes such as purification of natural gas, production of hydrogen-rich synthesis gas for manufacture of ammonia, alcohols, liquid fuels, cement and steel production and fermentation processes for food and drink production .

1.5 CO_2 separation technologies

The methods of CO_2 separation from flue gases, which are mainly applied in post-combustion capture system, as well as in capture from industrial processes, are based on physical and chemical processes, such as absorption, adsorption, membranes, cryogenic separation and chemical reactions (chemical looping) (Metz, B., Davidson, O., De Coninck, H., Loos, M., & Meyer 2005). Figure 5 shows an overview of the main CO_2 separation processes (Metz, B., Davidson, O., De Coninck, H., Loos, M., & Meyer 2005).

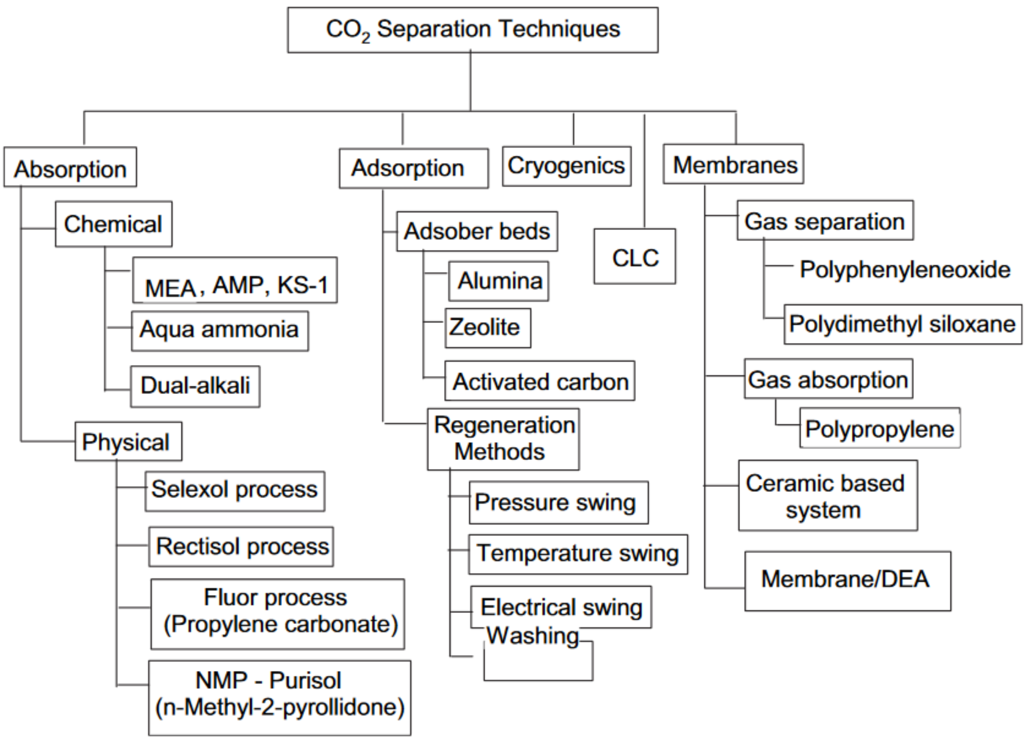

Figure 5: *Technology options for CO_2 separation.*

Chemical absorption processes typically use solutions of amines, e.g. MEA (Monoethanolamine). The stream of flue gases is bubbled through MEA solution, resulting in the formation of MEA carbamate. CO_2 and MEA are then regenerated by heating. The technique has some drawbacks, as it is highly energy intensive, it has a low CO_2 loading capacity and MEA is degraded by other components contained in flue gases such as SO_2, NO_2, HCl, O_2. Instead of MEA, other amines can be used, e.g. diethanolamine (DEA), or methyldiethanolamine (MDEA). The absorption with aqueous ammonia solution is possible, if other flue gases components are oxidized (SO_2 to SO_3, NO to NO_2), which results in a less energy demanding process (40% reduction respect with the MEA absorption) (Hunt et al. 2010). Physical absorption techniques are also applied, using e.g. dimethyl ethers of poly(ethylene glycol).

Adsorption techniques usually apply solid materials, such as activated carbons, molecular sieves, polymers, templated silicas, or other materials with strong affinity for CO_2 and with good adsorption/desorption capacity. Adsorption/desorption cycles are carried out by changing pressure (PSA - pressure swing adsorption) or temperature (TPA – temperature swing adsorption). This processes are generally considered low energy intensive and cost effective[12], but their drawback is due to high amounts of adsorbent required for the high volumes of flue gases in stationary power plants.

Another separation technique applies membranes, which allow the penetration of a specific gas through them. The driving force in membrane separation is usually a pressure difference, thus this technique is suitable for high pressure flue gases. Materials such as polymers, metals or ceramics found application as membranes in industrial processes to separate H_2 from flue gases, CO_2 or O_2. Membranes have not yet been applied for CO_2 capture on a large scale, due to problems with reliability and low cost required for CO_2 capture (Metz, B., Davidson, O., De Coninck, H., Loos, M., & Meyer 2005).

Cryogenic distillation, which is applied e.g. for O_2 separation from air, can be also used to separate CO_2 from flue gases. The process requires condensation of gas to liquid by a series of compression, cooling and expansion steps, and subsequent distillation (Metz, B., Davidson, O., De Coninck, H., Loos, M., & Meyer 2005). The drawback of this method is its high cost and high energy intensity. However, a high purity stream of CO_2 can be obtained.

CLC (Chemical Looping Combustion) technologies can be also applied for CO_2 separation (Hunt et al. 2010). They are relatively new methods, which are currently being developed. CLC processes require the application of metal oxides in e.g. NiO, CuO, Fe_2O_3 or Mn_2O_3 (oxygen carrier). The metal oxide is circulating between two reactors containing air and fuel, respectively. In the air reactor the carrier is oxidized and undergoes subsequent reduction in the fuel reactor, resulting in fuel oxidation and production of H_2O and CO_2. The stream of flue gases containing water and CO_2 is then dehydrated and compressed.

1.6 Utilization of CO_2 as a chemical feedstock

The perception of carbon dioxide on the scientific, societal and industrial levels has drastically changed during the last few decades. Carbon dioxide is no longer considered a harmful pollutant, but a valuable chemical and an important carbon source. The CO_2 capture and separation technologies, which are currently applied or are under development, can provide high purity CO_2 streams for the production of chemicals and fuels. There are already existing large-volume technological processes (refineries, ammonia production, ethylene oxide production, gas processing, H_2 production, liquefied natural gas, bio refineries), which can be considered as a source of pure CO_2 available for CCU technologies (Ampelli, Perathoner, and Centi 2015). CO_2 already finds a few number of applications. However, its use as chemical feedstock has still a huge potential, with a number of industrial opportunities and advantages, such as (Centi and Perathoner 2009) (Quadrelli et al. 2011):

- CO_2 becomes an interesting raw material with almost zero or even negative costs.
- CCU technologies can create a positive public image of companies as, with the increasing political and social pressure on reducing CO_2 emissions, carbon dioxide will be utilized to valuable products.
- Instead of inactive storage of carbon dioxide (CCS), CO_2 will be recycled. It will also reduce the costs of CO_2 transport.
- With the production of new chemicals, companies can gain new market shares.
- CCU gives opportunities to produce organic chemicals in a safer way, as many organic syntheses produce pollutants. For example, CO_2 is a 'green' alternative to toxic phosgene in organic synthesis of polycarbonates.

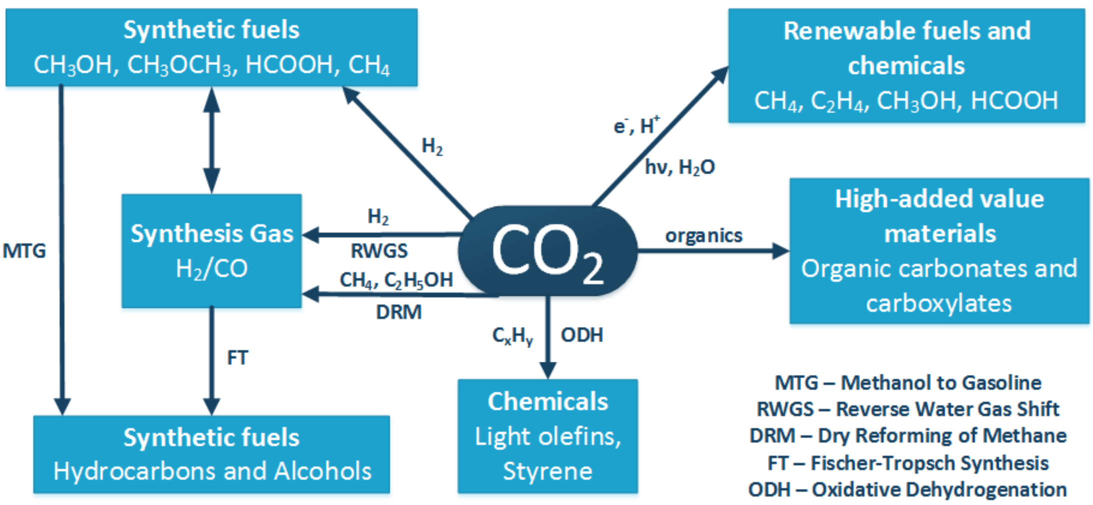

Figure 6: *Catalytic routes for CO_2 transformation into fuels and chemicals.*

Figure 6 (N. Homs, 2013) presents the current and potential technologies which use CO_2 for the production of synthetic fuels and added-value chemicals. It is predicted that processes involving CO_2 conversion will be developed on industrial scale in the coming decades, creating in this way a new carbon dioxide based economy (N. Homs, 2013). Since all of these reactions require the presence of catalysts, this clearly points to the importance of catalytic studies of these chemical reactions on laboratory and pilot scale. CO_2 conversion to fuels, rather than organic chemicals, is expected to play a major role in CO_2 emission management strategies. Firstly, because fuels market is much larger than the market of organic chemicals. Secondly, CO_2 emissions are mainly associated with the production of energy from fossil fuels. As reported by Centi et al. (Centi and Perathoner 2009) around 5-10% of current total CO_2 emissions is suitable for the production of fuels, which corresponds to reduction of ca. 1.75-3.5 Gt CO_2 emissions per year. As the processes of CO_2 conversion into fuels are energy demanding, there is a need to apply and develop renewable technologies in order to supply energy for these chemical reactions. Thus, carbon dioxide and CCU technologies are a key element of our sustainable development.

1.7 Hydrogenation of CO_2

CO_2 reduction is generally difficult because CO_2 possesses the highest oxidation state of carbon, and is thermodynamically stable and kinetically inert. The standard heat of formation of CO_2 is - 394.38 kJ/mol, and the C=O bond energy is 749 kJ/mol. Therefore, the reactions that generate reduced forms of CO_2 always require energy input and oxygen acceptors (Quadrelli et al. 2011), such as H_2, silane, borane and carbanion, etc. Because H_2 can nowadays be easily obtained from water, and the corresponding reduction process gives varieties of valuable products without generating much waste, the CO_2 hydrogenation technology has become one of the core technologies of CO_2 reduction and has been widely studied. The reactions of CO_2 with hydrogen offer various pathways for fuels and industrial chemicals production. Primary fuels and chemicals including carbon monoxide, formic acid, methane, methanol, higher hydrocarbons and oxygenates can be obtained through the CO_2 hydrogenation as shown in Figure 7 (Hu, Guild, and Suib 2013). These products can be produced through direct CO_2 hydrogenation or via an intermediate pathway. Several products generated from CO_2 hydrogenation are currently demanded in industrial quantities, due to existing infrastructure, while there is potential for other hydrogenation products to be demanded in similar quantities in the coming decades (Hu, Guild, and Suib 2013). Renewable energy sources, such as solar, wind, and hydroelectric energy, have been proposed as the energy source for CO_2 hydrogenation (Hu, Guild, and Suib 2013). Due to the kinetic stability of the CO_2 molecule, CO_2 hydrogenation requires efficient catalysts; these processes have historically utilized metal-based catalysts. Both homogeneous and heterogeneous catalysts have been used to hydrogenate CO_2 (Omae 2006). Homogeneous catalysts show satisfactory activity and selectivity, but the recovery and regeneration are problematic. Alternatively, heterogeneous catalysts are preferable in terms of stability, separation, handling, and reuse, as well as reactor design, which reflects in lower costs for large-scale productions (Omae 2006). The major challenge in CO_2 hydrogenation remains the development of stable catalysts able to perform a large scale process of CO_2 conversion to value added products. Therefore, there is a need for implementing laboratory experimentation and process design and simulation, both necessary to study the feasibility of these reduction processes.

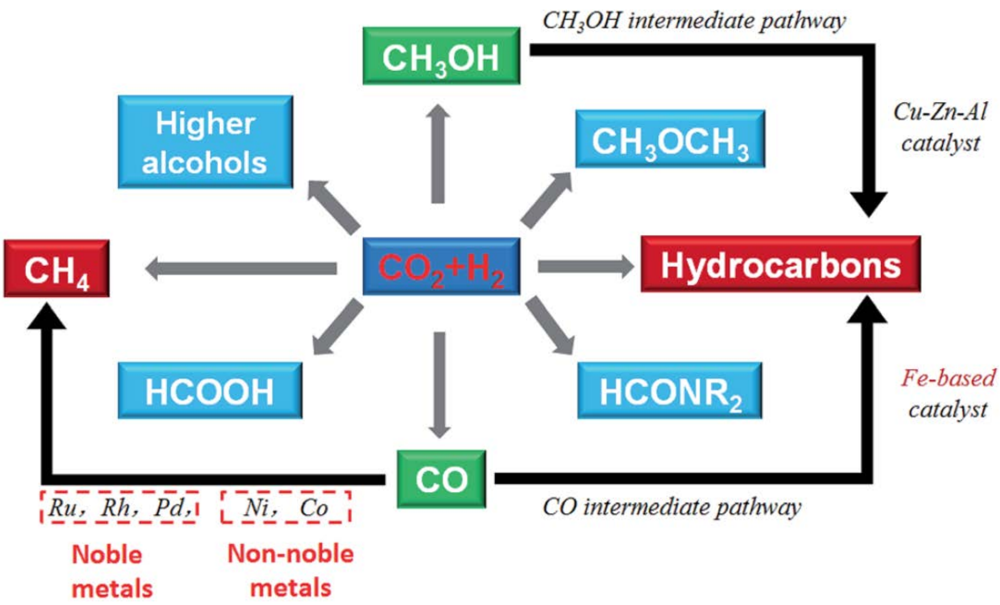

Figure 7: *Conversion of CO_2 to chemicals and fuels through CO_2 hydrogenation.*

1.8 Aim of the thesis

The aim of this thesis is to compare five different hydrogenation processes of carbon dioxide, in particular: methanol synthesis, methane synthesis, urea synthesis, syngas synthesis and formic acid synthesis. The processes are compared according to the following five technological parameters, defined based on the CO_2 treated in the processes.

$$\frac{\Delta CO_2}{CO_2{,}in} \tag{1.1}$$

The parameter indicated by the equation 1.1, the CO_2 conversion, is the key parameter in the CO_2 abatement. Its means is the percentage of CO_2 that has been converted into a new chemical therefore, its value should be close to 100 as much as possible.

$$\frac{H_2O}{CO_2,in} \qquad \left[\frac{ton\ H_2O}{ton\ CO_2,in}\right] \quad (1.2)$$

The second parameter, indicated by the equation 1.2, means the water that is produced per tonne of CO_2 treated in the process. The water produced from this hydrogenation processes is a secondary product that consume hydrogen, therefore, this parameter has been considered as an indicator of the formation of a secondary and worthless product that consume the reagent.

$$\frac{H_2}{CO_2,in} \qquad \left[\frac{ton\ H_2}{ton\ CO_2,in}\right] \quad (1.3)$$

The third parameter, indicated by the equation 1.3, means the hydrogen that is consumed per tonne of CO_2 treated in the process. This parameter is a direct indication for the comparison of the quantity of reagent that is necessary for the syntheses.

$$\frac{Therm.en.cons.}{CO_2,in} \qquad \left[\frac{MW_h}{ton\ CO_2,in}\right] \quad (1.4)$$

The fourth parameter, indicated by the equation 1.4, means the thermal energy consumption per tonne of CO_2 treated in the process. This parameter more than the others is the parameter that can be decide the feasibility or not of a synthesis in terms of energy therefore, for the process comparison, the optimization of this value is a prerogative.

$$\frac{Electr.cons.}{CO_2,in} \qquad \left[\frac{MW_h}{ton\ CO_2,in}\right] \quad (1.5)$$

The last parameter, indicated by the equation 1.5, means the electricity consumption per tonne of CO_2 treated in the process. This energy parameter, as the previous, can be considered as a metric for the processes sustainability comparison.

The processes investigated are divided into two main categories:

- Literature processes: based on academic publications in which process simulation results are reported, so that the technological parameters were retrieved/calculated from the available information.
- Designed processes: based on academic experiments and/or international patents, from which the reactions kinetics or the experimental conditions were derived, and implemented and simulated by Aspen Plus® simulation software. Process design was optimized with the aim of obtaining the highest conversion of carbon dioxide possible and the maximum recovery of the products, together with energy integration, in order to minimize the energy request and design an efficient process.

Obtaining the technological parameters for all the processes investigated, allows for a discussion of the results and a comparison between them. At the end, a summary of the main advantages and the critical issues of these CO_2 conversion processes is presented.

Chapter 2

Hydrogenation of CO_2: Literature processes

The second chapter discusses singularly three different academic works that simulate the hydrogenation of CO_2 to give different products. The methanol synthesis, the methane synthesis and the urea synthesis can be considered as processes with deep academic and industrial background; therefore, this chapter presents the state of art of processes that use CO_2 as a chemical feedstock, and for which simulation has already been carried out. The processes and the simulations are described in detail and the technological parameters are finally derived from the available simulation results.

2.1 Methanol synthesis

2.1.1 Introduction

Methanol (MeOH) is widely used in the chemical industry, mainly in the production of formaldehyde, methyl tert-butyl ether (MTBE) and acetic acid. The production of methanol is especially attractive in emerging economies, as a liquid fuel to replace conventional sources of energy. Methanol can be used in a wide range of concentrations mixed with gasoline, from small concentrations where it is an additive up to high concentrations such as the M85 (15% gasoline and 85% methanol), or even as pure methanol (M100). This versatility has led to the idea of the "methanol economy," proposed by Olah et al (Fuel Production with Heterogeneous Catalysis 2014). In the methanol economy, methanol replaces fossil fuels as a mean for energy storage, transportation, and raw materials for chemical production; in combination with CO_2 hydrogenation, the methanol economy represent a possibility for sustainable production and development.

2.1.2 Process reactions, kinetics and thermodynamics

The process simulation considered in this thesis is the one developed by Fortes et al. (Pérez-Fortes et al. 2016), that resulted highly detailed and compatible with our purpose. The simulation, implemented in CHEMCAD®, is based on the kinetic and thermodynamic information obtained by Van-Dal and Bouallou (Van-Dal and Bouallou 2012), which represents a detailed work concerning the CO_2 hydrogenation to methanol reaction study. This study assumes that the methanol process is governed by the two main reactions that occur in the reactor: equation 2.1 and equation 2.2.

$$CO_2 + 3H_2 \rightleftarrows CH_3OH + H_2O \qquad \Delta H_{298K} = -87\,\frac{kJ}{mol} \tag{2.1}$$

$$CO_2 + H_2 \rightleftarrows CO + H_2O \qquad \Delta H_{298K} = +41\,\frac{kJ}{mol} \tag{2.2}$$

While the first reaction is the one that produces MeOH, the second one is undesired because it consumes the feed meant for MeOH formation. The catalyst used for this synthesis is the tri-metallic $Cu/ZnO/Al_2O_3$, used also for the conventional methanol synthesis from syngas mixture. For this catalyst, the model proposed by Bussche and Froment (Bussche and Froment 1996) is able to describe with good precision the reactions of methanol production and the reverse water gas shift reaction (RWGS) (equation 2.2). The model assumes that CO_2 is the main source of carbon for the synthesis of methanol and that it does not cause direct inhibition of the reaction represented by equation 2.1, which was demonstrated by Sahibzada et al. (Sahibzada, Metcalfe, and Chadwick 1998). In addition, the model considers the inhibitory effect of water formed by the RWGS reaction. The activation energies of reactions were readjusted by Mignard and Pritchard (Mignard and Pritchard 2008) to better represent the experimental data, which also expanded the application range of the model up to 75 bar. Hence, the kinetic model used in the simulation is that of Bussche and Froment (Bussche and Froment 1996) with the readjusted parameters of Mignard and Pritchard (Mignard and Pritchard 2008) (equations 2.3 and 2.4, in which pressures are expressed in bar and temperatures in K). The kinetic constants follow the Arrhenius law (equation 2.5), and its parameters are summarized in Table 1 (Bussche and Froment 1996). The thermodynamic equilibrium constants are given by Graaf et al. (Graaf et al. 1986) (equations 2.6 and 2.7).

Methanol synthesis:

$$r_{CH_3OH} = \frac{k_1 P_{CO_2} P_{H_2}\left(1 - \frac{1}{K_{eq1}} \frac{P_{H_2O} P_{CH_3OH}}{P_{H_2}^3 P_{CO_2}}\right)}{\left(1 + k_2 \frac{P_{H_2O}}{P_{H_2}} + k_3 P_{H_2}^{0.5} + k_4 P_{H_2O}\right)^3} \qquad \left[\frac{mol}{kg_{cat}\, s}\right] \tag{2.3}$$

RWGS reaction:

$$r_{RWGS} = \frac{k_5 P_{CO_2}\left(1 - K_{eq2} \frac{P_{H_2O} P_{CO}}{P_{CO_2} P_{H_2}}\right)}{\left(1 + k_2 \frac{P_{H_2O}}{P_{H_2}} + k_3 P_{H_2}^{0.5} + k_4 P_{H_2O}\right)} \qquad \left[\frac{mol}{kg_{cat}\, s}\right] \tag{2.4}$$

Arrhenius law:

$$k_i = A_i exp\left(\frac{B_i}{RT}\right) \tag{2.5}$$

$$log_{10}K_{eq1} = \frac{3066}{T} - 10.592 \tag{2.6}$$

$$log_{10}\frac{1}{K_{eq2}} = -\frac{2073}{T} + 2.029 \tag{2.7}$$

Table 1: *A_i and B_i parameters values for the equation 2.5 [J/mol].*

k_1	A_1	1.07
	B_1	40,000
k_2	A_2	3453.38
	B_2	-
k_3	A_3	0.499
	B_3	17,197
k_4	A_4	$6.62*10^{-11}$
	B_4	124,119
k_5	A_5	$1.22*10^{10}$
	B_5	-98,084

2.1.3 Process simulation description

The methanol synthesis process can be divided into three different stages (Ott J., 2012) . In the first process stage, the feed gases are compressed up to the reactor feed pressure, using several compression stages with intercooling. In the second process stage, the pressurised feed is heated up and fed to the reactor. In the third process stage, MeOH is separated from water in a distillation column. The flowsheet of the process (Pérez-Fortes, Bocin-Dumitriu, and Tzimas 2014) is shown in Figure 9. The thermodynamic models used to perform the simulation are the Soave-Redlich-Kwong equation of state with modified Huron-Vidal mixing rules (SRK-MHV-2), used to calculate the thermodynamic properties of streams at high pressure (pressure > 10 bar) and the Non-Random-Two-Liquid activity coefficient model with the Redlich-Kwong equation of state (NRTL-RK) for the streams at low pressure (pressure < 10 bar). The CO_2 feed stream (1) is compressed through a four stage compressor with intermediate cooling. It is assumed that the CO_2 enters the system at 1 bar. The pressure increase of each compressor is approximately $(P_{out}/P_{in}) \approx 3$, leading to a final pressure of 78 bar (stream 9). The H_2 feed stream (8) is compressed with compressor 8 from 30 bar (assumed as the hydrogen release pressure of a water electrolysis equipment) up to 78 bar. Streams 9 and 10 are mixed with the compressed recycle stream (20) and fed to heat exchanger 10, where they heated up with a fraction of the reactor outlet stream (14), to reach the reactor inlet temperature of 210 °C. Reactor 11 is modelled as an adiabatic ideal plug flow reactor (PFR), according to the reaction kinetics (equation 2.1 and equation 2.2) discussed in section 2.1.2. The reaction rates are directly implemented in CHEMCAD®, and the amount of catalyst utilised is 44,500 kg of $Cu/ZnO/Al_2O_3$ with the characteristics summarised in Table 2 (Van-Dal and Bouallou 2012).

Table 2: *Characteristics of the $Cu/ZnO/Al_2O_3$ catalyst.*

Density	1775 kg_{cat}/m^3_{cat}
Particle diameter	5.5 mm
Fixed bed porosity	0.4

The obtained fixed bed volume is 42 m^3. As reported in Figure 8, the equilibrium of reactions 2.1 and 2.2 is reached almost half a way through the reactor. Therefore, a reduction of the mass of catalyst is possible, but it is not considered in the simulation.

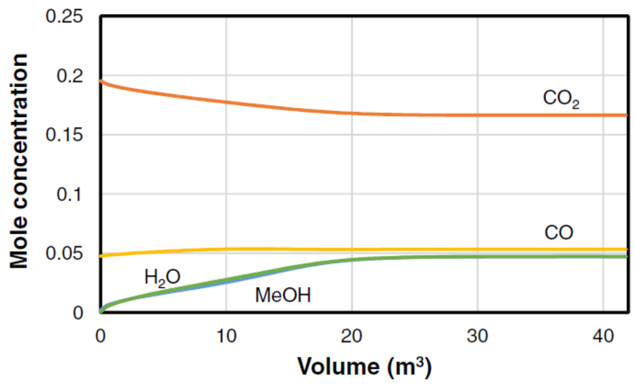

Figure 8: *Concentration profile for the different species along the PFR.*

Gaseous stream 13 leaves the reactor at 290 °C, with a MeOH content of 4.7 vol.%. The conversion of CO_2 into MeOH is around 21%. About 0.4% of the incoming CO_2 is converted to CO due to reaction equation 2.2. Stream 13 is divided into two streams. Stream 14, which is used to heat the reactor feed in heat exchanger 10, and stream 32, which is used in reboiler 22 that belongs to the distillation column (unit 21), and subsequently to preheat the feed to the column in heat exchanger 20. After this heat integration, the streams are mixed again and cooled down to 35 °C in heat exchanger 14, allowing for the condensation of almost all MeOH and water. Gas and liquid phases are then separated in flash vessel 18. Gas stream 18, which is mainly composed by H_2 and carbon oxides, is compressed and recycled back to the reactor. About 1% of the recycle stream is purged (stream 35) to avoid the accumulation of inert gases. The condensed liquid (21) is throttled to the pressure of 1.2 bar. The released gas is separated in another flash vessel (unit 19) and purged (stream 36). Condensate 23 is an almost gas-free mixture of MeOH and water with a MeOH concentration of $\xi_{CH3OH} \approx 63$ wt%. This mixture is preheated and partially evaporated in heat exchanger 20, using heat from the reactor off-gas. Then, the 2-phase stream is fed to the distillation column 21. This unit is modelled with 57 equilibrium stages, fed at stage 44 (counted from the top). A reflux ratio of 1.2 and a reboiler duty of 21.2 MW, are required to reach the design specifications of MeOH purity ($\xi_{H2O,top}$ < 100 wt ppm) and MeOH recovery ($\xi_{CH3OH,bottom}$ < 100 wt ppb) (Van-Dal and Bouallou 2012). Finally, product liquid MeOH (stream 31) leaves the process.

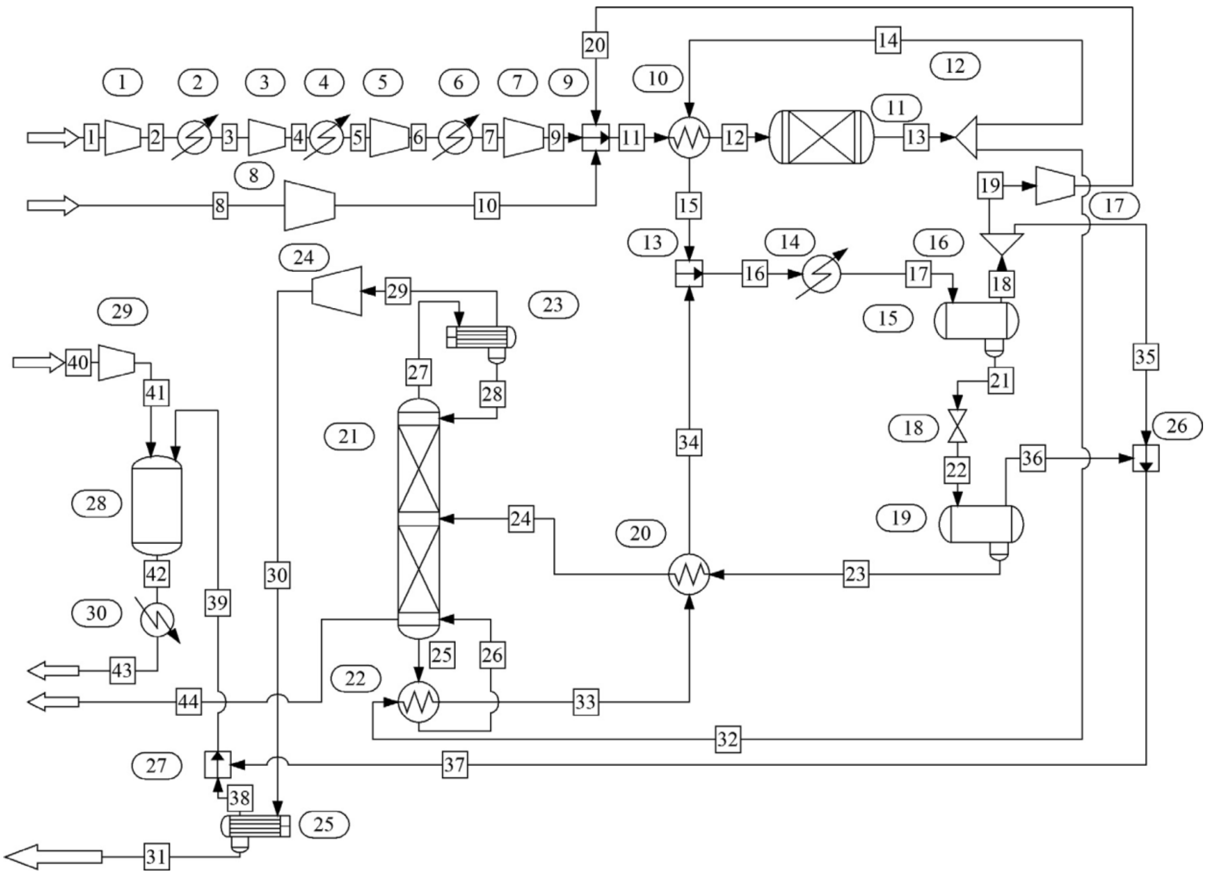

Figure 9: *Process flow diagram of the reference process.*

2.1.4 Reference simulation results

Table 3 summarizes the mass and energy balance resulting from the reference process simulation. The mass balance is expressed as tonne of reagent or product per tonne of methanol produced. Additionally, the CO_2 conversion in the reactor and in the process is reported. The energy balance is expressed as thermal energy consumption and electricity consumption, both per tonne of methanol produced.

Table 3: *Technological metrics evaluation for the MeOH synthesis.*

Mass balance (t/t$_{MeOH}$)	
Inlet CO_2	1.460
Inlet H_2	0.199
Outlet H_2O	0.569
CO_2 convR (%)	21.97
CO_2 convP (%)	93.85
Energy balance (MW$_h$/t$_{MeOH}$)	
Electricity consumption	0.169
Thermal energy consumption	1.301

The technological parameters are then calculated according to the reference simulation results as reported in the Table 4 (for the derivation see Appendix A).

Table 4: *Technological parameters calculated from the reference simulation results.*

$\Delta CO_2/CO_{2,in}$	**$H_2O/CO_{2,in}$**	**$H_2/CO_{2,in}$**	**Therm.en.cons./$CO_{2,in}$**	**Electr.cons./$CO_{2,in}$**
[-]	**ton H_2O/ton $CO_{2,in}$**	**ton H_2/ton $CO_{2,in}$**	**MW$_h$/ton $CO_{2,in}$**	**MW$_h$/ton $CO_{2,in}$**
0.938	0.390	0.136	0.891	0.116

2.2 Methane synthesis

2.2.1 Introduction

The CO_2 methanation reaction, also called the Sabatier reaction (equation 2.8), was first studied by Sabatier and Senderens at the beginning of the last century (Gahleitner 2013). Early use of the technology was to remove the trace of carbon oxides from the feed gas for the ammonia synthesis (Olivier et al. 2013)(Schmid 2015). Recently, the CO_2 methanation has gained renewed interest due to its application in the so called power-to-gas technology. In power-to-gas technology, the hydrogen produced from excess renewable energy is reacted with CO_2 (from power plants, industrial or biogenic processes) and chemically transformed to methane, which can be stored and transported through the well-developed natural gas infrastructure already in place. On the other hand, challenges related to implementation of the reaction still have to be resolved. The process parameters and catalyst affect the product yield. Considerable efforts have been devoted to investigate various aspects of CO_2 methanation ranging from the catalytic aspect to the process design and challenges related to its implementation. The catalysts developed today normally show high selectivity for CH_4, but improving the conversions at lower temperatures is still of importance.

2.2.2 Process reactions, kinetics and thermodynamics

The reference process considered for the methanation of CO_2 is the one developed by De Saint Jean et al. (De Saint Jean, Baurens, and Bouallou 2014). Their analysis is performed using the ProsimPlus 3™ simulation software. This work resulted as a thorough simulation present in literature, and it is based on the consolidated kinetic and thermodynamic study published by Lunde and Kester (Lunde and Kester 1974). Methane is produced thanks to the Sabatier reaction (equation 2.8). This is a catalytic and highly exothermal reaction which, when operating conditions are soundly chosen, can be considered as the unique possible chemical reaction between H_2 and CO_2 (Lunde and Kester 1974) (Gao et al. 2012).

$$CO_2 + 4H_2 \rightleftarrows CH_4 + 2H_2O \qquad \Delta H_{298K} = -165\,\frac{kJ}{mol} \tag{2.8}$$

Carbon dioxide and hydrogen can also react to form carbon monoxide and water thanks to the reverse-water-gas-shift reaction (equation 2.2) or carbon deposition (equation 2.9) (Gao et al. 2012).

$$2H_2 + CO_2 \rightleftarrows C_{(s)} + 2H_2O \qquad \Delta H_{298K} = -90.1\,\frac{kJ}{mol} \tag{2.9}$$

Other reactions are possible from these reactants to these products but they are linear combinations of the present ones. Thermodynamic analyses are used to determine the equilibrium state of a given mixture for a certain temperature T and pressure P. Lunde and Kester (Lunde and Kester 1974) studied the chemical equilibria involving H_2, H_2O, CO, CO_2, CH_4 and $C_{(s)}$ for temperatures ranging from 473 K to 1073 K and they found that, at atmospheric pressure and stoichiometric ratio between H_2 and CO_2, a temperature decrease promotes CH_4 production. Moreover, CO appears only at temperatures higher than 700 K. Below 700 K, only species involved in the Sabatier reaction are present. Carbon deposition has been observed when the reactants H_2 and CO_2 are in the ratio lower or equal to 3 (Lunde and Kester 1974). It should be mentioned that CH_4 selectivity is 100% provided that temperature is lower than 800 K and pressure higher than the atmospheric one. Therefore, in the frame of this study, the authors have operated with conditions chosen in such a way that CO and C(s) are not produced. Considering the effect of pressure, an increase involves higher CO_2 conversion, CH_4 yield and selectivity. Conclusions of these studies are that methanation of CO_2 is promoted by high pressure, low temperature and a stoichiometric ratio should be applied to optimise CH_4 production. With these conditions, CO and carbon deposition are absent from equilibrium compositions and CH_4 yield is maximised. These results legitimate the consideration of the Sabatier reaction on its own. This reaction is highly exothermal and catalytic, so a thermal management strategy is required to avoid high temperature which would lead to an acceleration of the catalyst sintering and deactivation (Kopyscinski, Schildhauer, and Biollaz 2010). The catalyst used in the simulation to determine the kinetics is ruthenium-based, which is a more promoting CO_2 hydrogenation catalyst compared to nickel-based one. However, due to progress on catalyst activity with less noble metals, it is expected to have in the near future nickel-based catalysts as good as this ruthenium-based catalyst. Lunde and Kester (Lunde and Kester 1974) studied the CO_2 methanation kinetics with the ruthenium-based catalyst. Studied kinetics are representative for the feed compositions $H_2/CO_2 = 4$ dilution. Catalytic tests were performed between 473 K and 643 K, at atmospheric pressure. The authors obtained the kinetic law (equation 2.10), where T is in K, P in MPa and n is an empirical pressure dependant constant whose discrete values are presented in Table 5 (Lunde and Kester 1974). The equilibrium constant, expressed with the partial pressure ratio in MPa, is calculated thanks to equation 2.11 at the standard pressure P^0.

$$\frac{dP_{CO_2}}{dt} = 1.792 * 10^8 * e^{-\frac{70524}{RT}} * \left(P_{CO_2}^n P_{H_2}^{4n} - \frac{P_{CH_4}^n P_{H_2O}^{2n}}{K_{eq.}(T^n)}\right) \qquad \left[MPa_{CO_2} * h^{-1}\right] \tag{2.10}$$

$$K_{eq.}(T) = 97.4 * \exp\left(\frac{28183}{T^2} + \frac{17430}{T} - 8.254 * lnT + 2.87 * 10^{-3} * T + 33.17\right) \tag{2.11}$$

Table 5: *n values according to the operating pressure P.*

P	Mpa	0.1	0.2	3.0
n		0.225	0.5	1

This kinetic expression is coherent with a Langmuir-Hishelwood mechanism expression where kinetic and adsorption/desorption effects are considered in the Arrhenius term, and the chemical driving force is taken into account in the second part of the expression. The value $n = 1$ has been taken as a first quite good approximation. After mathematical calculations, the kinetic law in $mol*s^{-1}m_{cat}^{-3}$ is given by equation 2.12, assuming that n equal to 1.

$$r_{CH_4} = 2.692 * 10^6 * e^{-\frac{64121}{RT}} * \left(P_{CO_2} P_{H_2}^4 - \frac{P_{CH_4} P_{H_2O}^2}{K_{eq.}(T)}\right) \tag{2.12}$$

2.2.3 Methanation reactor

Through the ProsimPlus 3™ software, a pseudo-homogeneous and one-dimensional equation system, or plug-flow, modelling approach has been applied to the modelled reactor illustrated schematically in Figure 10.

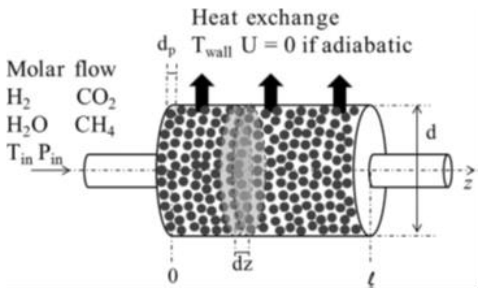

Figure 10: *Tubular reactor with catalytic fixed bed and boundary conditions.*

In this approach, three balances are used (Schlereth and Hinrichsen 2014): mass balance (equation 2.13), energy balance (equation 2.14) and momentum balance represented by the Ergun equation (equation 2.15), in the case where all parameters to describe the catalytic bed are known. In this equation set, *r* is the reaction rate in mol*$s^{-1}m_{cat}^{-3}$, and refers to the stoichiometric coefficient *v* of the species *i* in the chemical reaction to model, *Ω* is the reactor cross section, *U* the heat exchange coefficient (equal to 0 in the adiabatic case), *ρ* the gas density, *u* the fluid superficial velocity, *d* the reactor diameter, d_p the catalyst particle equivalent diameter, *α* the bed porosity and *μ* the fluid dynamic viscosity.

$$\frac{d\dot{n}_i}{dz} = \nu_i \times r \times \Omega \tag{2.13}$$

$$\frac{dT}{dz} = \frac{-r\Delta_r H(T)}{\sum_i^{n_{species}} C_{pi}\dot{n}_i} + \frac{4U(T_{wall}-T)}{d\sum_i^{n_{species}} C_{pi}\dot{n}_i} \tag{2.14}$$

$$\frac{dP}{dz} = 150\frac{(1-\alpha)^2}{\alpha^3}\frac{\mu u}{d_p^2} + 1.75\frac{(1-\alpha)}{\alpha^3}\frac{\rho u^2}{d_p} \tag{2.15}$$

The catalyst bed is characterised by the values summarised in Table 6. These data were measured at CEA-Liten on a commercial catalyst usually used for methanation. Catalyst particles are assumed spherical, with the equivalent diameter d_p.

Table 6: *Catalyst characterisation.*

d_p	mm	2.73
$\rho_{cat,bulk}$	kg/m^3	750
α		0.4

2.2.4 Process simulation description

The Soave-Redlich-Kwong (SRK) equation of state is chosen for the whole process simulation. The reference simulation is divided into three main section (Appendix B.1): the High-Temperature-Steam-Electrolysis unit (HTSE), where it is produced the pure stream of H_2; the methanation unit (Figure 11, adapted from (De Saint Jean, Baurens, and Bouallou 2014)) where the methanation of the CO_2 occurs; and the purification unit (Figure 12, adapted from (De Saint Jean, Baurens, and Bouallou 2014)) where the CH_4 is separated and the reagents are recycled back to the methanation process. Considering that the production of hydrogen is outside the boundaries of this thesis work, the HTSE unit has not been taken into account for the calculation of the technological parameters. Therefore, only the methanation unit and the purification unit were investigated. All the reactors used in the simulation are specified with the kinetic law 2.12. Reaction occurs in four adiabatic reactors in series, involving a temperature increase until being close to the chemical equilibrium, then the exiting gas is cooled-down to 573 K to feed the following reactor. Since H_2 and CO_2 sources are dissociated, and still to avoid high temperature, 95% of the CO_2 stream is sent to the first reactor, while the remaining fraction goes directly to reactor R2.

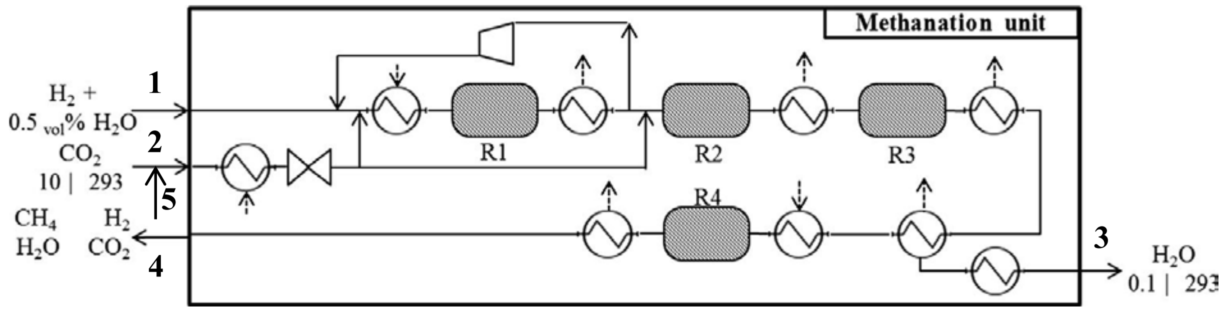

Figure 11: *Methanation unit, pressure in (MPa) and temperature in (K).*

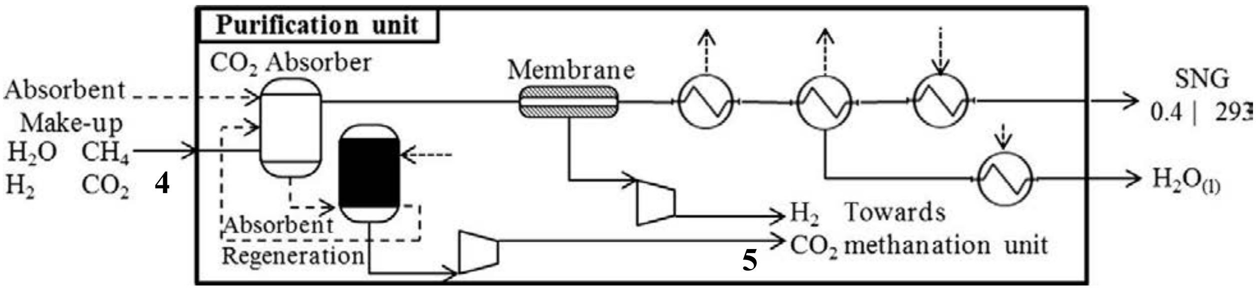

Figure 12: *Purification unit, pressure in (MPa) and temperature in (K).*

To limit the outlet temperature of reactor R1 at 820 K, a gas recirculation is set around reactor R1 at 75%. Finally, to improve the CO_2 conversion into CH_4, the equilibrium is displaced by removing water by condensation after reactor R3, and the gas containing CH_4, H_2 and CO_2 feeds the fourth and last reactor. This architecture allows to convert more than 95% of the incoming H_2 and CO_2.

2.2.5 Reference simulation results

Table 7, summarizes the parameters and the results obtained from the reference simulation for the methanation reactors, while Table 8 summarizes the streams results.

Table 7: *Parameters and results for the methanation reactors R1 to R4. d means the reactor diameter; L, the reactor length; V_{cat}, the volume of catalyst present in the reactor; Qin, the volumetric flow rate entering the reactor; χ_{CO2}, the CO_2 conversion in the reactor; ΔP, the pressure drop across the reactor; T_{out}, the temperature at the reactor outlet; P, the reactor thermal duty.*

	d	L	V_{cat}	Q_{in}	χ_{CO2}	ΔP	T_{out}	P
	m	m	m^3	Nm^3/h	%	kPa	K	kWth
R1	0.162	0.1	$2.05\ 10^{-3}$	1018	51.8	26.3	819	113.4
R2	0.187	0.7	$1.92\ 10^{-3}$	232.0	49.3	7.8	723	16.7
R3	0.350	5	$4.80\ 10^{-3}$	216.9	47.6	6.0	649	8.1
R4	0.350	2	$1.92\ 10^{-3}$	83.11	66.9	0.75	694	6.1
Total			$6.93\ 10^{-3}$		97.98	40.8		144.3

Table 8: *Physical values for streams 1 to 5, fractions (%) are molar. N, means the stream number, Q, the volumetric flow rate of the stream N_i; φ, the stream phase; T, the stream temperature; P, the stream pressure.*

N	Q	φ	T	P	H_2O	H_2	O_2	CO_2	CH_4
	Nm^3/h		K	MPa	%	%	%	%	%
1	263.8	g	301	0.74	0.5	99.5	0	0	0
2	66.4	g	303	0.74	0	0	0	100	0
3	126.4	l	293	0.10	100	0	0	0	0
4	77.7	g	293	0.44	7.21	6.94	0	1.74	84.11
5	0.3	g	476	0.78	1.00	0.02	0	98.63	0.36

In order to calculate the technological parameters, the streams are converted from Nm^3/h to ton/h and the total thermal and electrical energy consumption for the two sections is estimated (for the derivation see Appendix B.2). Finally, the technological parameters are estimated and the results obtained are reported in the Table 9.

Table 9: *Technological parameters calculated from the reference simulation results.*

$\Delta CO_2/CO_{2,in}$	$H_2O/CO_{2,in}$	$H_2/CO_{2,in}$	Therm.en.cons./$CO_{2,in}$	Electr.cons./$CO_{2,in}$
[-]	ton H_2O/ton $CO_{2,in}$	ton H_2/ton $CO_{2,in}$	MW_h/ton $CO_{2,in}$	MW_h/ton $CO_{2,in}$
0.985	0.801	0.183	0.595	0.122

2.3 Urea synthesis

2.3.1 Introduction

The urea is one of the most important and widely produced chemicals in the world. Based on the growing world population, the demand for crops and fertilizers has been large increased. Therefore, at the global level, the fertilizer industries became a highly concentrated market with increasing level of trade (Hernandez and Torero 2010). Among all common solid nitrogenous fertilizers, urea has the highest nitrogen content and for this reason, more than 90% of world industrial production of urea is used as fertilizer. It is also a raw material for many important chemical compounds like various plastics. Recently, the urea is used as a source of hydrogen, nitrogen and clean water in which provides safe, sustainable and long-term energy within valuable products (Rollinson et al. 2011). The production of hydrogen by electrolysis of a urea solution occurs at a lower voltage than water, therefore urea can be directly used as a source of hydrogen in fuel cells (Cowin et al. 2011). Urea is non-toxic, stable, and consequently easy to transport and store. The main industrial route for the urea production consists in the initially producing of ammonia (nearly all commercial production is based on the Haber-Bosch synthesis process) and a successive reaction with the carbon dioxide, normally produced from the natural gas (Pagani 1995).

2.3.2 Process reactions, kinetic and thermodynamic

The urea synthesis process considered in this section is the one developed by the Aspentech team (www.aspentech.com) that published a highly detailed and rigorous simulation of the process, developed in the Aspen Plus® process simulator. This simulation is based on the Stamicarbon CO_2 stripping process®, which is a popular and fast growing process for the manufacturing of urea. This process considers the two main reactions that take place in the urea synthesis process: reaction 1 (equation 2.16) and reaction 2 (equation 2.17).

$$CO_2 + 2NH_3 \rightleftarrows NH_2CO_2NH_4 \qquad \Delta H_{298K} = -117\,\frac{kJ}{mol} \tag{2.16}$$

$$NH_2CO_2NH_4 \rightleftarrows NH_2CONH_2 + H_2O \qquad \Delta H_{298K} = +15.5\,\frac{kJ}{mol} \tag{2.17}$$

The first reaction, which takes place in the liquid phase, converts the ammonia and carbon dioxide into ammonium carbamate (*CARB*). This reaction is highly exothermic and fast. Chemical equilibrium is readily reached under the operating conditions in the reactor (T = [167-183] °C; P = 138 bar). The second reaction also takes place in the liquid phase and it is endothermic. Its rate is slow and the equilibrium is usually not reached in the reactor. The kinetics of reaction 1 (equation 2.16) has been set to be very fast, so that equilibrium is effectively reached. The reaction kinetics has been formulated to approach the equilibrium composition for large residence times. The equilibrium has been described in terms of the fugacity coefficients, since an equation of state is used as the thermodynamic model. The equilibrium constant for reaction 1 (equation 2.16) is written as reported in the equation 2.18.

$$K_1 = exp\left\{\frac{-(G^0_{CARB}-2G^0_{NH_3}-G^0_{CO_2})}{RT}\right\}\left(\frac{P}{P^0}\right)^2\left[\frac{\phi^2_{NH_3}\phi_{CO_2}}{\phi_{CARB}}\right] \quad (2.18)$$

Where: T = temperature; P = pressure; x = mole fraction vector; R = gas constant; P^0 = reference pressure (1 atmosphere); $G^0{}_i$ = Ideal-gas Gibbs free energy of component i at T, P^0; ϕ_i = fugacity coefficient of component i at T, P, x. The equilibrium constant for reaction 1 in terms of mole fractions results therefore as reported in equation 2.19.

$$K_1 = \frac{x_{CARB}}{x^2_{NH_3}x_{CO_2}} \quad (2.19)$$

Similar equilibrium equations can be written for reaction 2. The rates for the two reactions are then derived and reported in the equations 2.20 and 2.21, in units of kmol/s/m^3.

$$r_1 = k_1\left\{x^2_{NH_3}x_{CO_2} - \frac{x_{CARB}}{K_1}\right\} \quad (2.20)$$

$$r_2 = k_2\left\{x_{CARB} - \frac{x_{UREA}x_{H_2O}}{K_2}\right\} \quad (2.21)$$

The rate constant for reaction 2 determines the urea conversion in the reactor. The model applied for the thermodynamic properties calculation of the NH_3-CO_2-H_2O-UREA-CARBAMATE-N_2-O_2 system is the SR-POLAR model within Aspen Plus®. The model uses an equation of state and is thus suitable for the high pressure and high-temperature conditions of urea synthesis. Furthermore, the model contains extensions that enable an accurate description of the phase and chemical equilibria, the density and the other thermodynamic properties (e.g., enthalpy) of this system. A user subroutine USURA.f, developed by the authors, include the reaction kinetics of both reactions. USURA.f is used in the reactor simulations and both forward and reverse reactions are considered.

2.3.3 Process simulation description

The reference process is depicted in Figure 13. Feed CO_2 is compressed and fed to the CO_2 stripper E01, to strip the urea solution coming from the reactor. In the stripper (RADFRAC with 10 stages), ammonium carbamate decomposes, liberating more NH_3 and CO_2 to be stripped out. Heat is supplied on the shell side of tubes by condensing 20 bar steam, while the urea solution falls inside the tubes counter-currently down past the rising CO_2 stripping gas. The outlet liquid solution from the stripper is rich in urea and goes to the downstream section for the urea purification (modelled as an RStoich reactor working at T = 72,4 °C, P = 138 bar and a SEP). In the adiabatic urea reactor, R01 (T = [167-183] °C; P = 138 bar), an aqueous solution of NH_3 and CO_2 (much in the form of ammonium carbamate) and vapours flow upward through 8 stages of reactor volume to minimize back-mixing and provide enough residence time for the urea formation (τ = 0.44 h). Remaining gases condense and carbamate decomposes in the reactor to provide heat for the slightly endothermic reaction of carbamate to urea. The urea solution overflows from the top of the reactor and back to the stripper E01, while the unreacted gases pass out the top of the reactor. These unreacted gases are sent to the scrubber E03 (RADFRAC with 5 stages), where recycled carbamate solution from the Evaporation/Recirculation section (S13) is passed over the top of a packed bed and fills the tube side section of vertical tubes. The gases rise up through the tubes and pass up through the packed section before leaving the top of the vessel. The contact with the carbamate solution absorbs the unreacted NH_3 and CO_2, while the inert gases N_2 and O_2 (S15) are vented out from the top. The bottom solution of the scrubber E03 together with the top vapour stream from the stripper E01 is fed to the carbamate condenser E02.

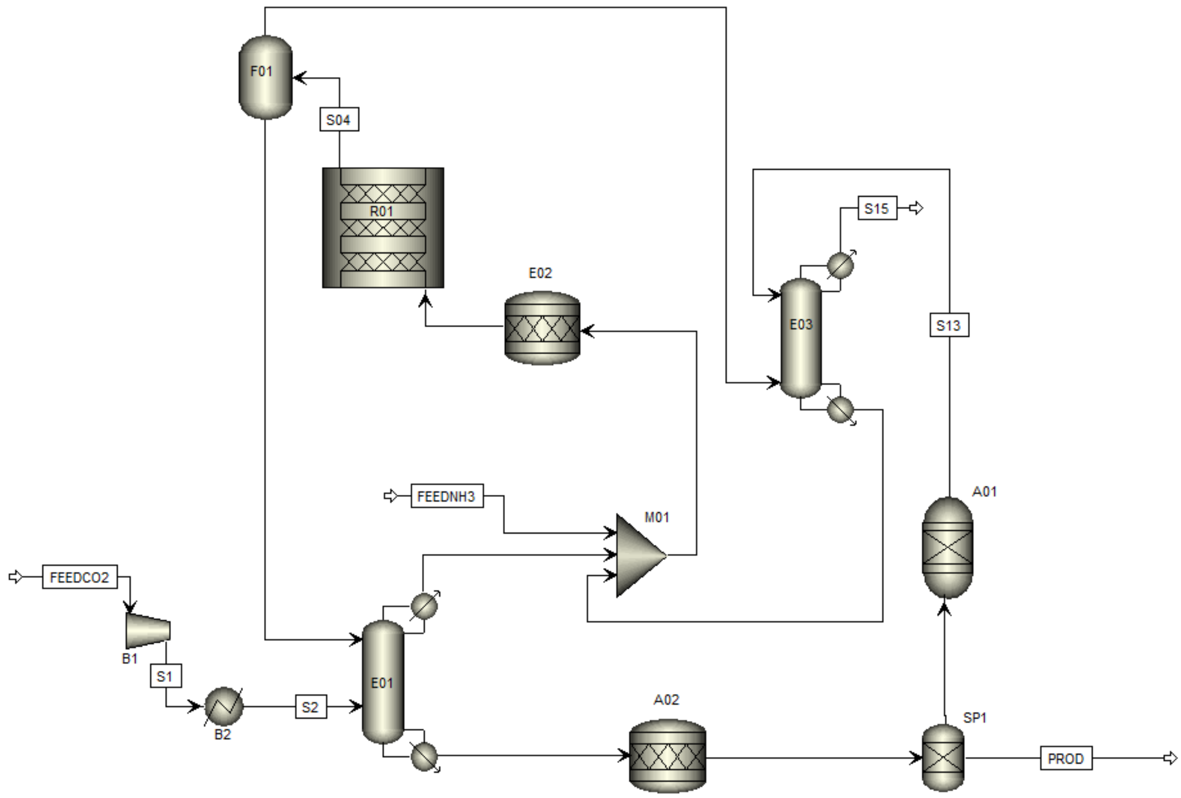

Figure 13: *Flowsheet of the reference process simulation for the urea synthesis.*

2.3.4 Reference simulation results

As the process simulation considered takes into account the reaction of CO_2 with NH_3, in order to obtain the corresponding hydrogen consumption of the urea synthesis, the hydrogen necessary to produce the ammonia feed required for the urea synthesis was evaluated. The reference is the well known Haber-Bosch (www.aspentech.com) process. Accordingly, it has been taken into account also the thermal and electrical consumption necessary to produce the ammonia feed required for the synthesis (for the derivation see Appendix C). Finally, the technological parameters for the urea synthesis are estimated and the results obtained are reported in the Table 10.

Table 10: *Technological parameters calculated from the reference simulation results.*

$\Delta CO_2/CO_{2,in}$	**$H_2O/CO_{2,in}$**	**$H_2/CO_{2,in}$**	**Therm.en.cons./$CO_{2,in}$**	**Electr.cons./$CO_{2,in}$**
[-]	**ton H_2O/ton $CO_{2,in}$**	**ton H_2/ton $CO_{2,in}$**	**MW_h/ton $CO_{2,in}$**	**MW_h/ton $CO_{2,in}$**
0.996	0.412	0.137	4.571	0.955

Chapter 3

Syngas synthesis

The third chapter investigates the hydrogenation of CO_2 to produce a syngas mixture. The scientific literature of this hydrogenation process is very limited. Therefore, the study of this process and its simulation are built step by step according to the only, but detailed, patent that has been found in literature. The reaction model, the thermodynamics and the relative assumptions are deeply discussed in the first subchapters. The approach to the simulation and its implementation are then explained and discussed and, at the end, the energy integration of the simulated process is applied. Finally, the technological parameters are estimated from the results.

3.1 Introduction

The syngas is a gaseous mixture containing hydrogen (H_2) and carbon monoxide (CO), which may further contain other gas components like carbon dioxide, water, methane, and/or nitrogen. In the past decades, numerous processes have been developed to produce the synthesis gas, which can be considered one of the most important feedstocks in the chemical industry. The natural gas and light hydrocarbons are the predominant starting material for making this mixture. The syngas is successfully used as synthetic fuel and also in a number of chemical processes, such as the synthesis of methanol or ammonia, Fischer-Tropsch type and other olefin synthesis, hydroformulation or carbonylation reactions, reduction of iron oxides in steel production, etc. The idea of substituting the natural gas or the light hydrocarbons with the pure CO_2 and H_2 as chemical feedstocks for the syngas synthesis has become nowadays a promising field of research. The CO_2 hydrogenation through the well-known RWGS (equation 2.2 of Chapter 2, here proposed again) gives the possibility to obtain the same syngas mixture obtainable from the conventional petrochemical processes. Therefore, its study and implementation can be considered as a sustainable process for the CO_2 abatement and transformation from a waste material to a new chemical platform. The syngas synthesis developed in this thesis has been build up according to the European patent specification EP 2 152 409 B1 (Tepzz 2016). Starting from the experimental data reported by the authors, it has been possible to develop a model used in the reactor of the simulation. The reaction is as follows:

$$CO_2 + H_2 \rightleftarrows CO + H_2O \qquad \Delta H_{298K} = +41\,\frac{kJ}{mol} \qquad (2.2)$$

3.2 Patent description

The invention refers to a catalytic process for the production of the syngas mixture from pure carbon dioxide, more specifically, to a process of making a syngas mixture containing hydrogen, carbon monoxide and carbon dioxide, comprising a step of contact of a gaseous feed mixture containing carbon dioxide and hydrogen with a metal oxide based catalyst. The patent discloses the process of CO_2 hydrogenation in the gas phase in the presence of a catalyst composed of manganese (Mn) oxide and metallic chrome (Cr), supported on alumina (Al_2O_3). The catalyst comprises at least one alkali metal, e.g. lithium (Li), which further suppresses the coke formation, and thus improves catalyst stability and life-time. It should be mentioned that the catalyst developed in this patent does not contain iron (Fe), which is normally used as catalyst in the conventional syngas synthesis process. Iron should be avoided to suppress the formation of methane via the so-called methanation side-reactions (equation 2.13 proposed in the second chapter). Formation of methane as a by-product is generally not desired, because not only it means that less CO is being produced, but also because it may reduce the catalyst lifetime by accompanied formation of coke and deposition thereof. The object of the patent is therefore to provide a catalyst that shows improved selectivity in reducing carbon dioxide with hydrogen into the syngas mixture, with good catalyst stability, and especially able to suppress methanation reaction. The authors state also that the product mixture obtained has an amount of methane less than 0.1 vol%, or even below the detection limit of the gas chromatography equipment used for the on-line analysis of the product stream. The process thus shows a very high selectivity towards the syngas mixture, more specifically to the formation of CO with CO selectivity typically higher than 99% or even 99.5%. A further advantage of this invention is that the reaction can be performed over a wide pressure range, and particularly at atmospheric conditions, at which the CO selectivity can be maintained just as high. The stoichiometric number SN (defined as: SN = $([H_2]-[CO_2])/([CO]-[CO_2])$) of the syngas mixture obtained can also be varied over a wide range, e.g. by varying the composition of the feed mixture. SN can, for example, vary from 0.5 to 3.0, making it possible to obtain syngas mixtures of different composition, to be used as raw material in the synthesis of various other products like alkanes (e.g. ethane, propane and iso-butane), aldehydes, ethers (e.g. dimethylether) or alcohols (e.g. methanol). The resulting product of this CO_2 hydrogenation process is a gas mixture containing carbon monoxide and water, non-converted carbon dioxide and the excess of hydrogen. This can be represented by the equation:

$$CO_2 + n\,H_2 \rightleftarrows CO + (n-1)\,H_2 + H_2O \qquad (3.1)$$

The water formed in this reaction is then removed from the product stream, so as to drive the equilibrium reaction in the desired direction, and because water is often interfering with subsequent reactions of the syngas. The amount of hydrogen in the feed gas, that is the value of n in the above reaction, may vary widely, for example from n = 1 to n = 5, to result in a syngas composition, expressed as H_2/CO ratio or as the stoichiometric number (SN), which can consequently vary within wide limits. The advantage is that the syngas composition can be adjusted and controlled to match the desired use requirements. Hence, the experiments reported from the authors, that are summarized in Table 8, start from different CO_2/H_2 mixtures in order to study also the possibility to obtain different CO/H_2 product mixtures. Considering that the reaction is endothermic, a high temperature will promote the CO_2 conversion, but a too high temperature may also induce the unwanted reactions. Accordingly to this last consideration, the experiments reported in Table 11 have been performed by the authors at a temperature ranging from 530 to 700°C and at atmospheric pressure, in the presence of 1%Li-10%Cr-8%Mn-O/Al_2O_3 catalyst. The tests have been performed in a laboratory glass tube filled with about 1 ml of catalyst to make a fixed bed type of reactor, and placed vertically inside a temperature-controlled oven. The authors reported the different feed compositions tested at different temperatures and the corresponding composition of the products obtained, on a dry basis, measured after a period of time of 1 hour or more through the use of a gas chromatography.

Table 11: *Experimental data obtained by the authors. The feed composition is expressed as vol%. T is the reaction temperature. t is the time, expressed in minute, before the measurement. The product composition is express as vol%.*

Feed composition (%vol)		**T**	**t**	**Product composition (%vol)**		
CO_2	**H_2**	**°C**	**min**	**CO_2**	**H_2**	**CO**
52	48	680	60	40.5	40.2	20.5
33.8	66.2	680	60	21.7	59.7	18.5
33.8	66.2	700	120	22.5	58.5	18.9
23	77	580	60	12.8	74.5	12.7
23	77	580	300	12.9	73.8	13.2
23	77	580	420	12.9	74	12.9
23.5	76.5	530	60	13.4	74.1	12.5
23.5	76.5	580	60	14.2	75.4	10.4

3.3 Reaction model derivation

Considering the absence of sufficient information to develop a detailed kinetic model of this synthesis, it was decided to regress a linear model from the experimental data proposed by the authors. The goal of this regression model is therefore to replace the kinetic model of the process with a prediction of the outputs of the reactor based on the input variables. The regression has been developed through the use of a Partial Least Square (PLS) regression. The PLS is a method for constructing predictive models when the factors are many and highly collinear. The main objective is to predict the responses and not necessarily trying to understand the underlying relationship between the variables. The PLS is used to find the fundamental relations between two matrices (**X** and **Y**), i.e. a latent variable approach to modelling the covariance structures in these two spaces. A PLS model will try to find the multidimensional direction in the X space that explains the maximum multidimensional variance direction in the Y space (Barker and Rayens 2003). The general underlying model of the multivariate PLS is reported by the equations:

$$\boldsymbol{X} = \boldsymbol{T}\boldsymbol{P}^{\boldsymbol{T}} + \boldsymbol{E} \tag{3.2}$$

$$\boldsymbol{Y} = \boldsymbol{U}\boldsymbol{Q}^{\boldsymbol{T}} + \boldsymbol{F} \tag{3.3}$$

Where **X** is an $n\times m$ matrix of predictors, **Y** is an $n\times p$ matrix of responses; **T** and **U** are $n\times l$ matrices that are, respectively, projections of **X** (the X score, component or factor matrix) and projections of **Y** (the Y scores); **P** and **Q** are, respectively, $m\times l$ and $p\times l$ orthogonal loading matrices; and matrices **E** and **F** are the error terms, assumed to be independent and identically distributed random normal variables. The decompositions of **X** and **Y** are made so as to maximise the covariance between **T** and **U**. The PLS model consists of a simultaneous projection of both the **X** and **Y** spaces on a low-dimensional hyperplane. The matrix of the predictor **X** and of the responses **Y** used to calibrate the model has therefore been isolated from the experimental data reported by the authors.

$$\boldsymbol{X} = \begin{array}{c} \begin{array}{cccc} \boldsymbol{CO_2} & \boldsymbol{H_2} & \boldsymbol{T} & \boldsymbol{t} \end{array} \\ \begin{bmatrix} 52 & 48 & 680 & 60 \\ 33.8 & 66.2 & 680 & 60 \\ 33.8 & 66.2 & 700 & 120 \\ 23 & 77 & 580 & 60 \\ 23 & 77 & 580 & 300 \\ 23 & 77 & 580 & 420 \\ 23.5 & 76.5 & 530 & 60 \\ 23.5 & 76.5 & 580 & 60 \end{bmatrix} \end{array} \qquad \boldsymbol{Y} = \begin{array}{c} \begin{array}{ccc} \boldsymbol{CO_2} & \boldsymbol{H_2} & \boldsymbol{CO} \end{array} \\ \begin{bmatrix} 40.5 & 40.2 & 20.5 \\ 21.7 & 59.7 & 18.5 \\ 22.5 & 58.5 & 18.9 \\ 12.8 & 74.5 & 12.7 \\ 12.9 & 73.8 & 13.2 \\ 12.9 & 74 & 12.9 \\ 13.4 & 74.1 & 12.5 \\ 14.2 & 75.4 & 10.4 \end{bmatrix} \end{array} \tag{3.4}$$

The PLS regression has been used therefore to estimate the matrix of the β_i coefficients **B** for a linear regression between the **X** and **Y** experimental data as in equation:

$$\boldsymbol{Y} = \boldsymbol{X}\boldsymbol{B} + \boldsymbol{B_0} \tag{3.5}$$

For our case, $\mathbf{B_0}$ has been set equal to zero, considering the limited set of experiments used for the regression, and to eliminate the bias. The PLS regression has been realized through the use of the MATLAB® software. The resulting matrix of the coefficients necessary to predict the outputs in a linear manner resulted as in the equation:

$$\boldsymbol{B} = \begin{array}{c} \boldsymbol{\beta_1} \\ \boldsymbol{\beta_2} \\ \boldsymbol{\beta_3} \\ \boldsymbol{\beta_4} \end{array} \begin{bmatrix} 0.3390 & -0.3458 & 0.3247 \\ -0.3390 & 0.3458 & -0.3247 \\ 0.2918 & -0.2976 & 0.2794 \\ -0.1115 & 0.1137 & -0.1086 \end{bmatrix} \tag{3.6}$$

In Figure 14 the Q residual vs. T^2 and the Y measured vs. the Y predicted are shown for the PLS regression. The regression predicts the Y variables with a good accuracy: the first principal component explains 92 % of the Y variability with 71 % of the variability of X.

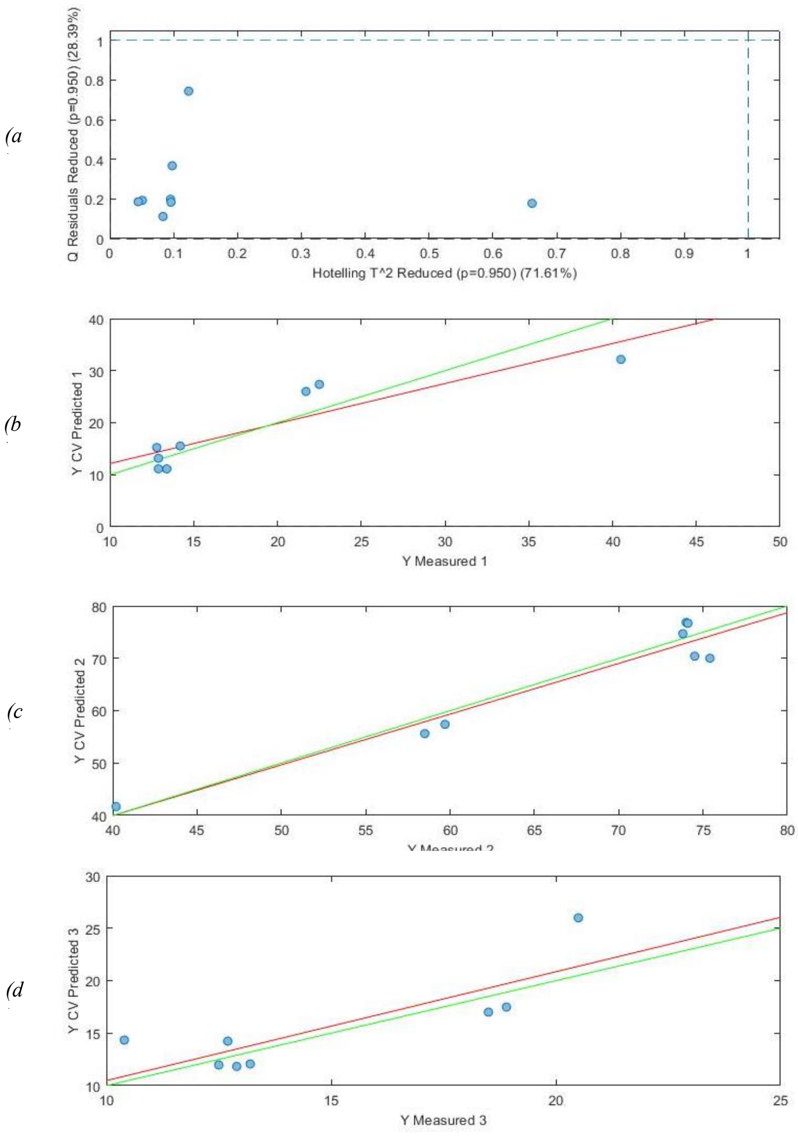

Figure 14: *PLS regression results: (a) Q residual vs. T^2; (b) Y measured 1 vs. the Y predicted 1; (c) Y measured 2 vs. the Y predicted 2; (d) Y measured 3 vs. Y predicted 3.*

Once the **B** matrix of the coefficients is calculated, and thanks to an experimental inlet row vector **x** = [x_{CO2}, x_{H2}, x_T, x_t], the linear model can predict the output vector **y** = [y_{CO2}, y_{H2}, y_{CO}] according to the **B** matrix founded as follows:

$$\boldsymbol{y} = \boldsymbol{xB} \tag{3.7}$$

3.4 Simulation approach

The simulation of the process was developed through the use of Aspen Plus V9® process simulator. At the beginning, the simulation was started by adding the four components involved in the chemical reaction (CO_2, H_2, CO and H_2O) and by selecting the thermodynamic approach. The thermodynamic model has been selected considering that the reaction occurs at atmospheric pressure. Therefore, the NRTL method has been considered as a good approximation for the system considered. Moreover, the gases (CO_2, H_2, CO) were defined as Henry components. The reactor was modelled as a stoichiometric unit (*RStoic*) where the reaction (equation 2.2) has been specified together with the synthesis temperature and pressure (1 atm). The CO_2 conversion evaluation has been applied through the use of a calculator block, by writing a calculation code (Appendix D.1) that solves the linear equation 3.7 starting from the four reactor inlet information (**x** = [x_{CO2}, x_{H2}, x_T, x_t]), and calculates the three outputs (CO_2, H_2, CO). These are normalized accounting for the H_2O produced, which was set equal to the CO predicted), as discussed in the section 3.3 of this chapter. It must be noted that the reaction time (x_t) was imposed, because it cannot be entered as a variable in the simulation. Therefore, its optimized value (in the dataset) has been considered as a constant in the calculator block. Considering this approximation, it was decided to perform the simulation with the dataset optimized conditions, this in order to convert the maximum CO_2 possible. Accordingly, a mixture composed by 23% of CO_2 and 77% of H_2 (on molar basis) has been set by a design specification, to be the feed of the reactor. Finally, a reactor temperature of 530 °C and a residence time of 60 minute was imposed. The process design has been developed with the aim of converting the maximum amount possible of the CO_2 entering the process thus, a pressurized water absorption/desorption of the CO_2 from the reaction products has been sized in order to recycle the highest amount possible of the unreacted CO_2, and to purify the products. At the end, the energy integration of the process, better known as pinch analysis, has been evaluated and put in practice into the simulation, with the objective of saving the maximum thermal energy possible and reduce the energy consumption.

3.5 Simulation description

3.5.1 Base case description

The base case of the simulation designed is depicted in Figure 15. The pure CO_2 feed gas (1.5 ton/h) is assumed to be available at atmospheric pressure and ambient temperature, and enters the process after mixing with the material recycle, which contains also the required amount of H_2. A design specification is added in the mixer M1 in order to manipulate the inlet flow rate of CO_2 so to obtain the decided feed mixture of the reactor (23% of CO_2 and 77% of H_2). The reactor feed mixture is thus heated in the heat exchanger HE1 to the reaction temperature (530 °C). It is assumed to operate the stoichiometric reactor in an isothermal manner at the reaction temperature. The calculator, at this point, predicts with the trained model the output composition of the products that are immediately cooled down to 100 °C in the heat exchanger HE2. At this point, the purification of the products and the recycle of the reactants has been designed. Among the different solvents available for the CO_2 absorption, and considering that this study has been developed in such a way to be as ‘green’ as possible water has been chosen as the ideal solvent for this process, also considering that it is produced from the reaction itself. The study has been carried out considering the absorption of the CO_2 in water at 25 °C. The CO_2 recovery has been set to be equal to 97.5 percent and therefore, to make it reliable, a sensitivity analysis has been done to study the amount of water needed to achieve this result. Considering that the flow rate of water at 1 bar to achieve this goal resulted to be very high, another sensitivity analysis was performed to study the effect of the pressure in reducing the water flow rate, respecting anyway the design specification desired. The result of this study is depicted in the Figure 16.

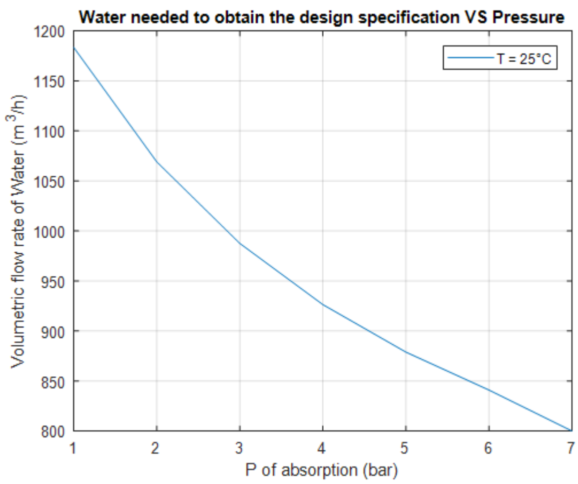

Figure 16: *Sensitivity analysis for the study of the pressure effect on the water reduction needed to obtain the design specification.*

It has been considered that the pressure of 7 bar was good compromise between the water consumption and the increasing of the energy consumption. Therefore, another sensitivity analysis was carried out to evaluate the CO_2 recovery in the liquid phase as a function of the inlet water flow rate, for an absorption column operating at 7 bar, as shown in Figure 17.

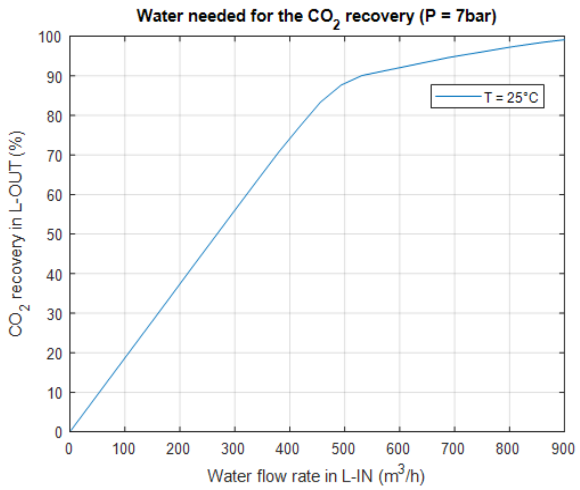

Figure 17: *Sensitivity analysis for the study of the water needed to obtain the desired design specification at P = 7 bar.*

The desired specification is then realized through an absorption tower made of 12 equilibrium stages, with a volumetric water flow rate 817.530 m^3/h. The compressed reactor products meets therefore in counter-current the water flow and a solvent make up that is added to respect the CO_2 recovery design specification imposed. The 1.35 ton/h of gas extracted from the top of the column, consists in a syngas mixture with a H_2/CO ratio equal to 2.5, which presents traces of water that are eliminated through the use of a separator (SEP1). The resulting syngas mixture contains an amount of CO_2 that is equal to 0.03 % (on mass basis). The water rich in CO_2 gas is then sent to a desorption column that works at 1 bar, with the aim of regenerating the solvent. A gas stream made by pure H_2 (0.266 ton/h), that represents also the hydrogen inlet of the process, has been decided to be the gas phase of the desorption (stripping) column. This solution has been developed in order to obtain an outlet gaseous recycle stream made only by a mixture of the reactants, whose molar ratio is later adapted through the design specification of the mixture M1 to be the desired one for the reactor. It must be noted that with this technical solution the only species involved in the process simulation are the ones that participate in the chemical equilibrium therefore, the purification of the product and of the recycle can be realized with less equipment than in a process using different solvents and stripping gases. Stripping with air resulted instead in the presence of substantial amounts of N_2 and O_2 not only in the recycle stream, but also in the purified syngas product, making this choice unfeasible. Thus, the H_2 stripping gas meets counter-currently the water rich in CO_2 liquid stream.

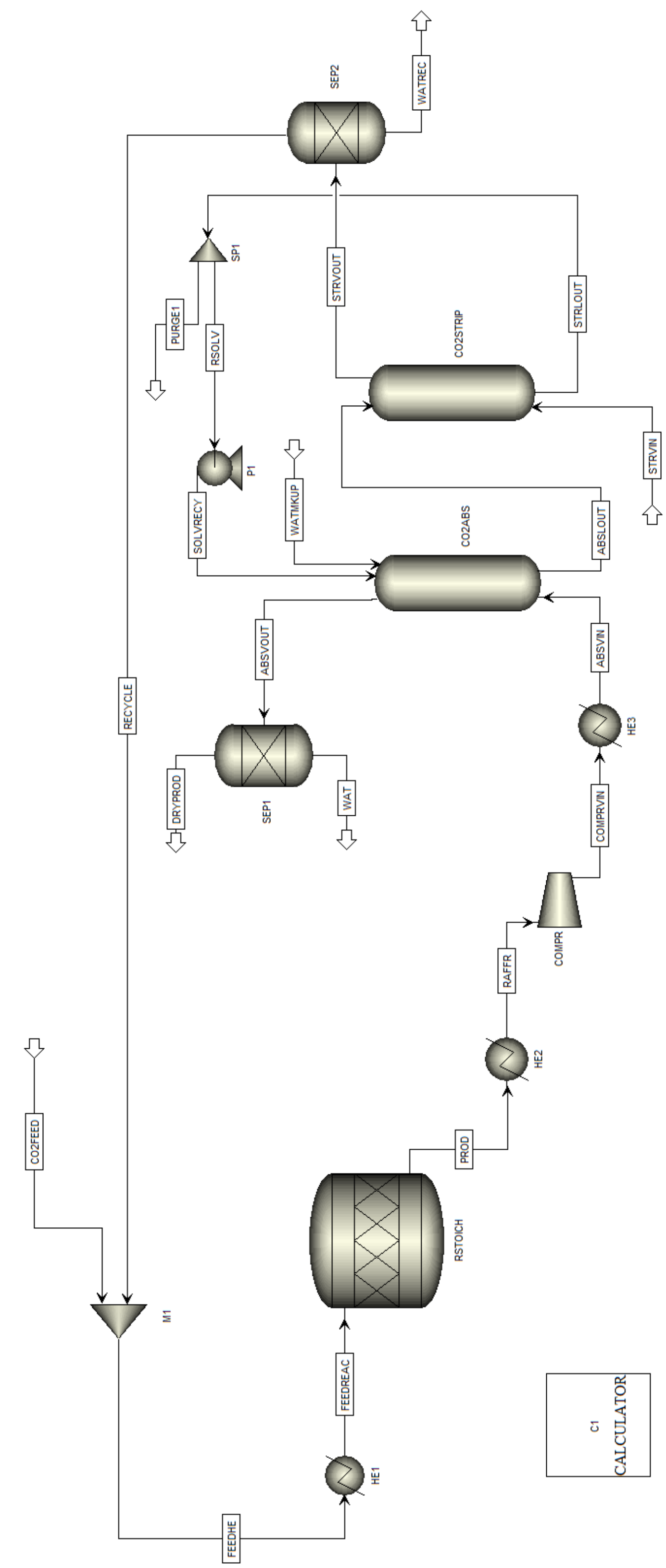

Figure 15: *Flowsheet of the base case of the Syngas synthesis process simulated.*

The solvent regeneration is realized by adding to the simulation a design specification that manipulates the H_2 feed gas streamin order to recover the 98 % of the CO_2 in the top gas product of the column. This specification is achieved through the use of two equilibrium stages. Once the water is purified, a pump re-compress the water to 7 bar to recycle it in the absorption column. A second separator (SEP2) is finally added to remove the traces of water from the recycle stream.

3.5.2 Integrated process description

Considering the endothermal behaviour of the process and the high temperature at which is performed, an energy integration results necessary to reduce the thermal energy requirement and save the maximum thermal energy possible. This study has been realized through the use of the Aspen Plus V9® energy analyser tool. The software calculates the hot and cold composite curves and the grand composite curve, both realized assuming a 10 °C delta T minimum approach.

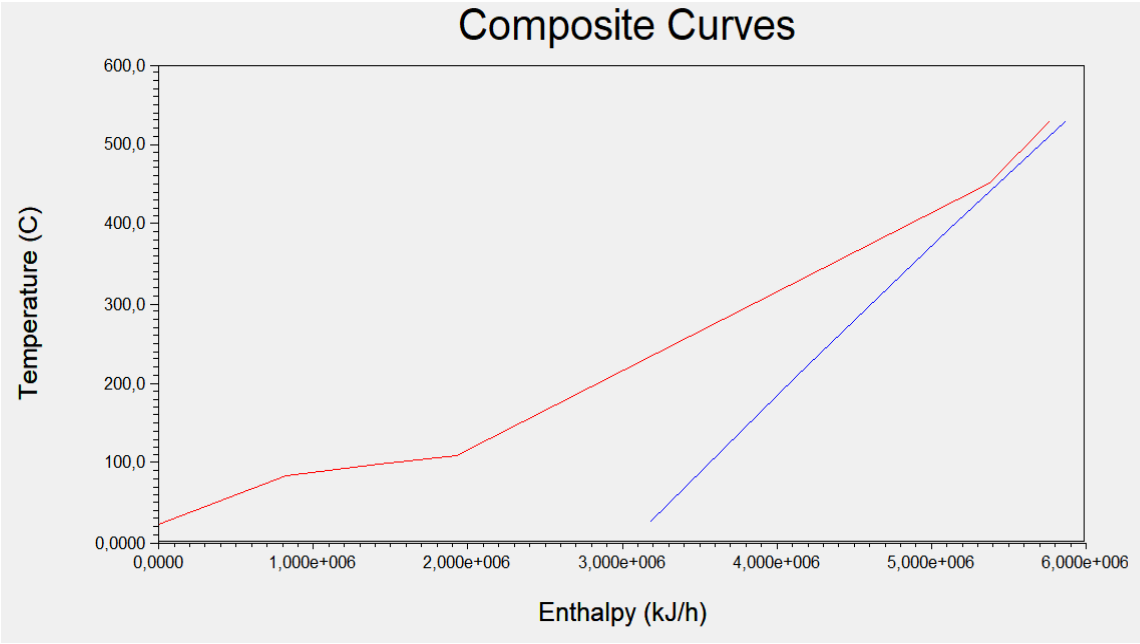

Figure 18: *Composite curves of the simulated process, realized with a delta T min approach of 10 °C. The red curve represent the hot composite curve while the blue, the cold composite curve.*

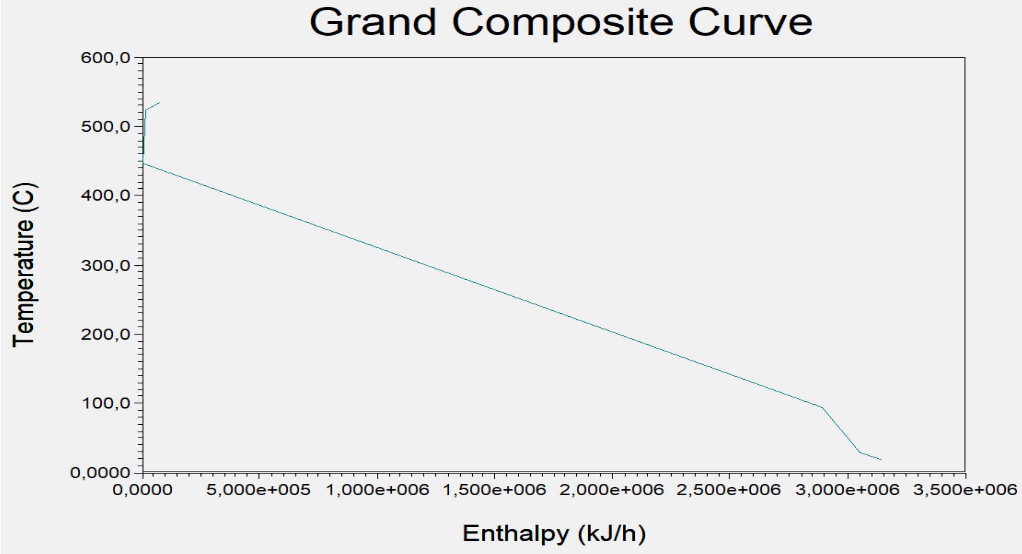

Figure 19: *Grand composite curves of the simulated process, realized with a delta T min approach of 10 °C.*

From Figure 18 and Figure 19, it can be observed that a good amount of energy can be saved, therefore the heat exchangers of the process simulated have been integrated into a network in order optimize the consumption and exploit the process interactions. Once the network has been build, the only heat to be provided to the process is represented by the hot and cold duty. The network built for the simulated process is shown in Figure 20 and finally, the resulting process flowsheet obtained after the energy integration is reported in Figure 21.

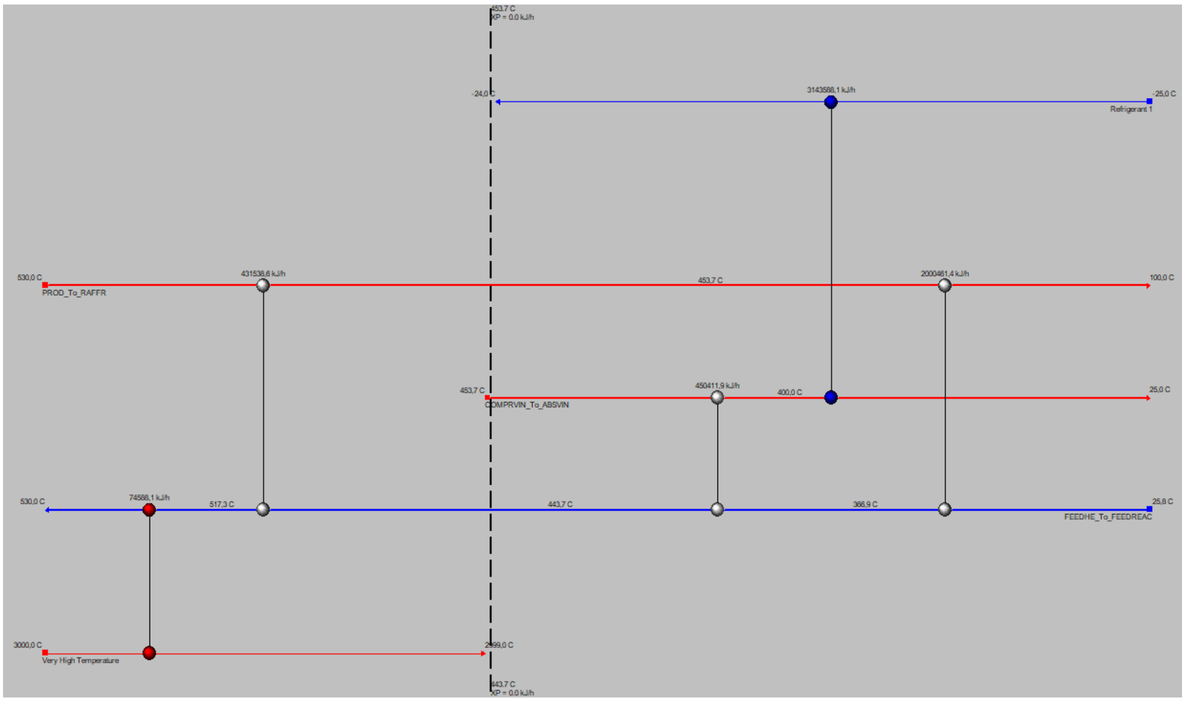

Figure 20: *Heat exchangers network designed for the simulated process. The red line represent the hot streams and the blue represent the cold streams. The red dots and the blue dots represent the hot and the cold duty that must be added to realize this network into the process simulation.*

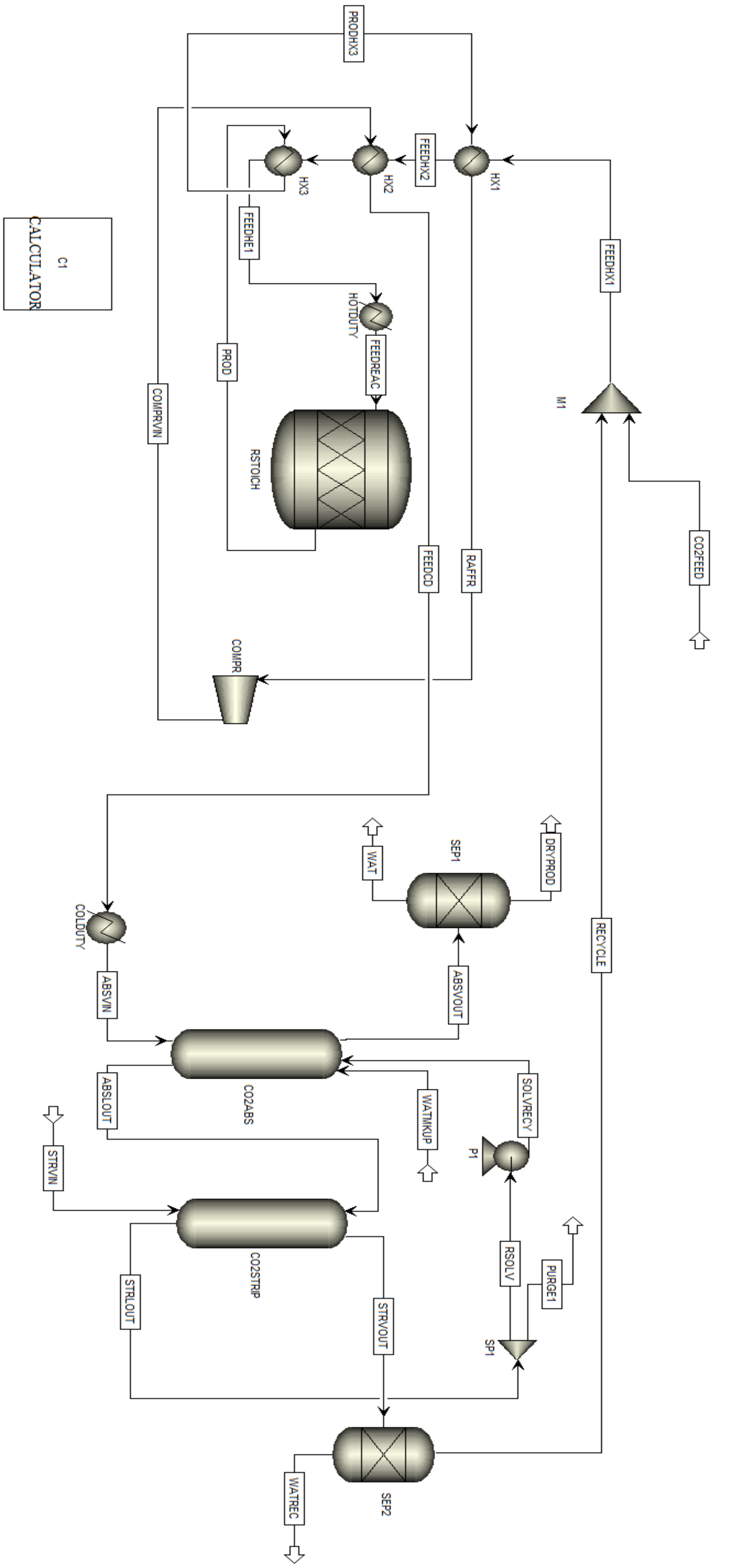

Figure 21: *Flowsheet of the integrated process for the Syngas synthesis process simulated.*

3.6 Simulation results

The results obtained from the integrated process simulation are summarized in Table 12 and are written in the form of the technological parameters needed for the final processes comparisons (for the derivation, see Appendix D.2).

Table 12: *Simulation results obtained for the integrated process simulation of the Syngas synthesis.*

$\Delta CO_2/CO_{2,in}$	**$H_2O/CO_{2,in}$**	**$H_2/CO_{2,in}$**	**Therm.en.cons./$CO_{2,in}$**	**Electr.cons./$CO_{2,in}$**
[-]	**ton H_2O/ton $CO_{2,in}$**	**ton H_2/ton $CO_{2,in}$**	**MW_h/ton $CO_{2,in}$**	**MW_h/ton $CO_{2,in}$**
0.997	0.408	0.162	0.787	0.430

The 1.35 ton/h of syngas produced resulted with a H_2/CO ratio equal to 2.5, this ratio permit to use this mixture directly in the Fischer-Tropsch process for the synthesis of alkanes and alcohols. Finally, it must be noted that the integrated process allows to reduce the thermal energy request of the base case simulation process from 2.834 MW to 1.181 MW. Therefore, the energy integration of the process, allows to reduce the thermal energy requirement of about 58 %.

Chapter 4

Formic acid synthesis

The fourth chapter investigates the hydrogenation of the CO_2 to formic acid. As for the syngas mixture investigated in the Chapter 3, the process of formic acid synthesis from pure CO_2 is not widely investigated in the literature. This study is therefore realized based on the only two works concerning this process that were found in literature: an academic article which studies the kinetics of this reaction and a patent, based on the same article. At the beginning, the kinetic model and its parameters are estimated and optimized and after that, the thermodynamic approach used for the simulation and its assumptions are deeply discussed. Later, it is introduced the study of the reactor and its rigorous implementation in the process simulator. Finally, the simulation results are discussed, together with the limitations of the thermodynamic approximations done and the future works necessary to improve this process simulation.

4.1 Introduction

Formic acid (FA) is widely used as preservative, insecticide, and industrial material for synthetic processes. It can be also used directly in FA fuel cells to provide electricity. Most recently, it is recognized as one of the most promising hydrogen storage materials, especially for portable power application, because of its many advantages: it is (1) nontoxic and biodegradable; (2) liquid at ambient conditions; (3) easy to store and transport; (4) it has a relatively high hydrogen content (4.4 wt%) and (5) it is highly sustainable and renewable. Considering these benefits, the study and the implementation of a sustainable process for the hydrogenation of CO_2 to formic acid becomes nowadays a challenge. The formic acid synthesis developed in this chapter is based on the kinetic study proposed by Jessop et al. (Thomas et al. 2001). This study proposes a reaction system consisting of CO_2 and H_2 gases, liquid triethylamine, an additive, and a catalyst precursor. The triethylamine (NEt_3) serves as a base, which stabilizes the formic acid product as a 2:1 adduct as reported in the following equation:

$$CO_2 + H_2 + 0.5NEt_3 \xrightarrow[RuCl(O_2CMe)(PMe_3)_4]{} 0.5[HCO_2H]_2NEt_3 \tag{4.1}$$

The role of the additives is known to accelerate the reaction in the supercritical phase (Thomas et al. 2001). In the study proposed by the authors, a water-methanol mixture was chosen among the different additives, thanks to its capability to affect the reaction rate most significantly with respect to others. The catalyst precursor used for this synthesis is the complex $RuCl(O_2CMe)(PMe_3)_4$.

$$0.5[HCO_2H]_2NEt_3 \xrightarrow{vacuum} HCOOH + 0.5NEt_3 \tag{4.2}$$

The adduct of formic acid and tertiary amine can be later thermally dissociated into free formic acid and tertiary amine (equation 4.2) and therefore, it serves as intermediate in the preparation of formic acid.

4.2 Kinetic model and parameters estimation

The rate law and the synthesis conditions have been obtained according to the experimental information given by Jessop et al. (Thomas et al. 2001). The authors reported three different sets of experiments performed in a 31 mL vessel under the following conditions: T = 50 °C, 0.5 h reaction time, 2.5 mmol of MeOH, 3.6 mmol of NEt_3 and 3.0 mmol of $RuCl(O_2CMe)(PMe_3)_4$. The study focused on the effect of the partial pressure of the two reagents on the turnover frequency (TOF), (i.e. mole of formic acid per mole of catalyst per hour).

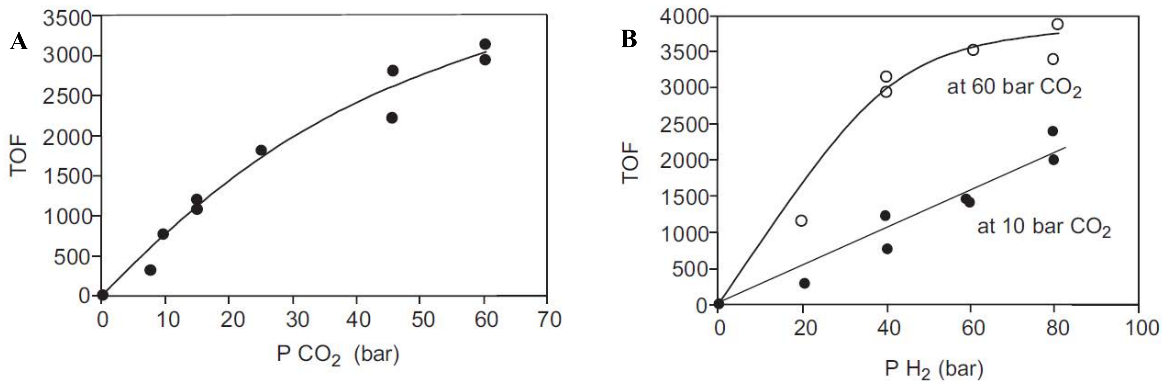

Figure 22: *(A) Dependence of the rate of CO_2 hydrogenation, express as TOF [h^{-1}], on the pressure of CO_2 at 40 bar H_2; (B) Dependence of the rate of CO_2 hydrogenation, expressed as TOF [h^{-1}], on the pressure of H_2 at 10 and 60 bar CO_2.*

According to Figure 22 A, that refers to a constant partial pressure of H_2 of 40 bar, the authors found that at lower partial pressures of CO_2 the rate is first-order with respect to CO_2, while the order declines somewhat at higher pressure. In Figure 22 B, the rate dependence on the H_2 partial pressure was measured at two different partial pressures of CO_2. At 10 bar of CO_2, it has been found that the rate is first-order with respect to H_2, while at 60 bar of CO_2 the rate shows a saturation kinetics with respect to H_2 (i.e., it is first-order at low H_2 pressure and lower order at higher pressure). The authors finally report the rate law that represents the experimental data obtained:

$$\frac{d[HCOOH]}{dt} = \frac{k_4 k_2 [H_2][CO_2][Ru_{tot}]}{1+k_2[CO_2]} \tag{4.3}$$

In equation 4.3, the rate is expressed as moles of formic acid over time, while $[H_2]$ and $[CO_2]$ represent the partial pressures of the two reagents and are expressed in bar; $[Ru_{tot}]$ represents the molar concentration of the catalyst and finally, k_2 and k_4 are the two kinetic constants, both expressed in $bar^{-1}h^{-1}$. Considering that the authors did not provide the values of the kinetic constants, it has been decided to estimate them through the use of the experimental results depicted in Figure 22. First, the coordinates of the experimental data and the relative TOFs have been retrieved, and are reported in Table 13.

Table 13: *Experimental data extracted from the Figure 22. The first two column correspond to the data extracted from the Figure 22 A, the others, from the Figure 22 B.*

40 bar H_2		**10 bar CO_2**		**60 bar CO_2**	
TOF (h^{-1})	**pCO_2 (bar)**	**TOF (h^{-1})**	**pH_2 (bar)**	**TOF (h^{-1})**	**pH_2 (bar)**
0	0	0	0	0	0
350	7.5	300	20.5	1150	20
800	9.5	750	40	2950	40
1075	15	1200	39.5	3100	40
1200	15	1400	60	3500	61
1825	25	1450	59	3300	80
2225	45.5	2000	80	3900	81
2800	46	2400	80	-	-
2900	60.5	-	-	-	-
3100	60.5	-	-	-	-

At this point, it has been isolated the definition of TOF from the rate law provided by the authors as reported in equation 4.4.

$$\frac{d[HCOOH]}{dt[Ru_{tot}]} = TOF = \frac{k_4 k_2 [H_2][CO_2]}{1+k_2[CO_2]} \tag{4.4}$$

However, it should be noted that the rate low provided was not able to fit the experimental data at 60 bar of CO_2 because, due to the linear dependence on $[H_2]$, it gave a straight line. To overcome this problem, after several attempts done with the process modelling software gPROMS®, it has been derived the best fitting function (TOF′) of the experimental data:

$$TOF' = \frac{k_4 k_2 [H_2][CO_2]}{1+(k_2[CO_2])^{(n[H_2])}} \tag{4.5}$$

In equation 4.5, n represents an empiric factor added in order to obtain the best fitting of the experimental data. The three unknown parameters (k_2; k_4; n) were therefore estimated through the gPROMS® software, which implements the maximum likelihood method to estimate the parameters of a statistical model. The results obtained from the parameters estimation are summarized in Table 14. There are not statistics for this parameters estimation because there was using single experiments with single points.

Table 14: *Result obtained from the parameters estimation done through the use of the software gPROMS®.*

k_2	k_4	n
0.049542	72.97050	0.015337

The results of the model described by equation 4.5 with the estimated parameters are illustrated in Figure 23.

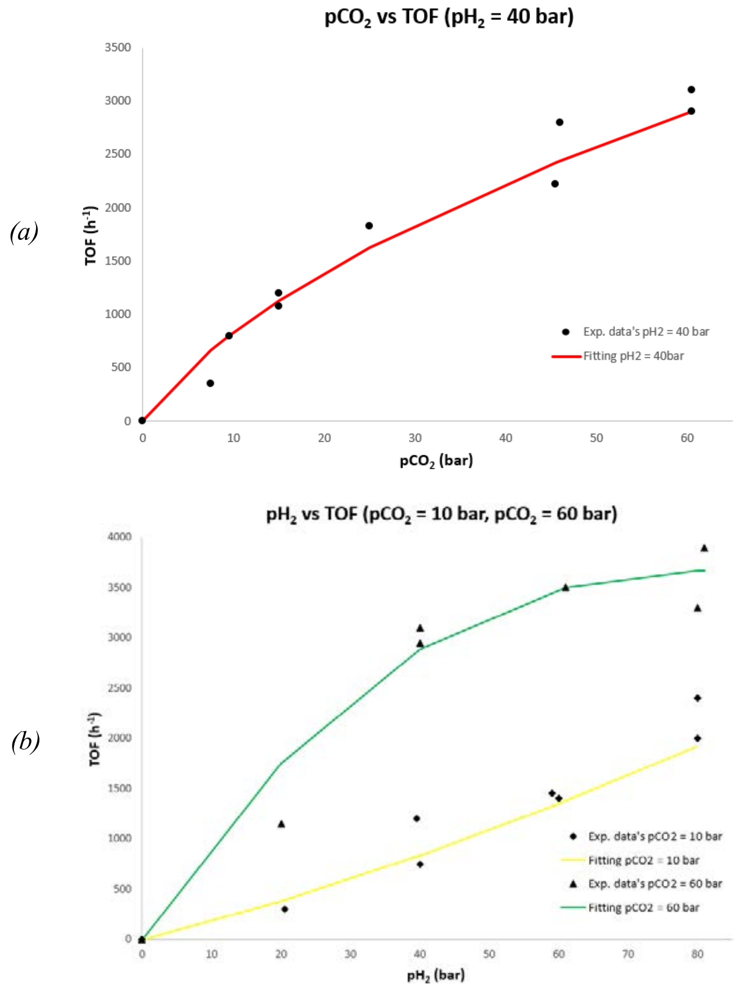

Figure 13: *(a) Fitting obtained with the estimated parameters for the pH_2 = 40 bar; (b) Fitting obtained with the estimated parameters for the pCO_2 = 10 bar (yellow curve) and pCO_2 = 60 bar (green curve).*

4.3 Thermodynamic approach

In order to push the reaction to the product it has been decided to operate the reactor at high pressure, to obtain a high TOF and thus, a high CO_2 conversion. The thermodynamic approach used in the simulation of this process has been therefore divided into two main categories, based on the operating pressure of the stage of the process. For the process units operating at high pressure (P > 3 bar in our case) it has been decided to use the Predictive-Soave-Redlich-Kwong (PSRK) equation of state, for its capability of estimate the properties of mixtures which contain supercritical components (P = 105 bar in our case). For the low pressure equipment, it has been implemented the NRTL model, with the Hayden-O'Connell equation of state for the vapour phase (NRTL-HOC). The Hayden-O'Connell method has been chosen for its high capability of describe the equilibrium involving polar and non-polar compounds (in particular systems with carboxylic acids), which is a prerogative for the separation stages of this simulation. Also, the H_2 and the CO_2 have been defined as Henry components, to better describe their solubility. At the beginning of the study, the matrix of the NRTL binary interaction parameters present in the database (NIST ThermoData Engine of the Aspen Plus® process simulator) was checked, to verify the presence of all the parameters required to perform a reliable simulation. This matrix is summarized in Table 15.

Table 15: *Matrix of the binary interaction parameters found in the NIST. "-" means the interaction with itself; Henry means the components declared as Henry component; v means that the binary interaction parameters are present in the NIST; x means that the binary interaction parameters are not present in the NIST.*

	CO_2	H_2	HCOOH	H_2O	CH_3OH	NEt_3
CO_2	-	Henry	x	v	v	v
H_2	Henry	-	x	v	v	x
HCOOH	x	x	-	v	x	x
H_2O	v	v	v	-	v	v
CH_3OH	v	v	x	v	-	v
NEt_3	v	x	x	v	v	-

Due to the absence of the binary interactions of more than one couple, some assumptions were made in order to retrieve the missing parameters of the matrix and complete it. The assumptions are based on the molecular similarity between the components the missing couples with other components whose parameters are instead present in the database. Once a suitable substitute has been identified, its binary parameters have been overwritten in the missing couple empty file of Aspen Plus®. In particular, the missing couples: CO_2-HCOOH, H_2-HCOOH and CH_3OH-HCOOH have been replaced with the interactions of: CO_2-Acetic acid, H_2-Acetic acid and CH_3OH-Acetic acid present in the database. For the couple NEt_3-H_2, since, among all the amines present in the Aspen database, only a few were found for which the interaction parameters with H_2 were available, the normal-propylamine (N-Propylamine) was chosen as the best candidate for the replacement. For the last missing couple, i.e. the HCOOH-NEt_3 couple, the binary vapour-liquid equilibrium of this mixture at 1 bar was found in the work by

(K Narita, 1975). The experimental results obtained by the authors have been loaded in the Aspen Plus® property analysis, and the binary interaction parameters were regressed with the NRTL model. The result of this regression is depicted in the Figure 24.

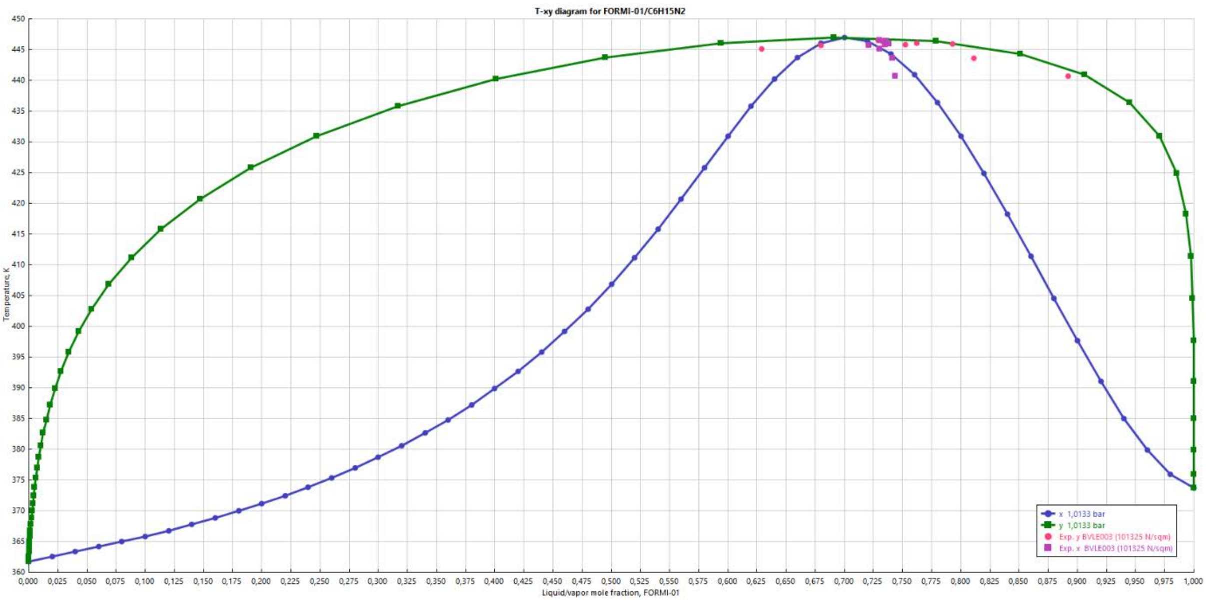

Figure 24: *Result of the regression from the experimental data[47] with the vapour liquid equilibrium.*

The parameters found with this regression have been thus imported in the property matrix. At this point, all the thermodynamic information necessary to describe the equilibrium are present and then the property analysis is launched.

4.4 Reactor study and simulation approach

Considering the unconventional rate law of equation 4.5, its application in the Aspen Plus® process simulator requires to import it by means of a user subroutine (Appendix C.1). The subroutine, must be written in Fortran® code to be interpreted from the process simulator. The Fortran® code must therefore be written in the codes editor Visual Studio® to be ready to be traduced in a standard code for the process simulator. Once created the file.f in Visual Studio®, from the prompt of the commands of Aspen Plus®, the file is converted into a subroutine available for the simulation, that is called from the reactor block and is solved during the process simulation. It has been decided to implement the reaction in a Continuous Stirred Tank Reactor (CSTR), this in order to perform a process closest as much to the one reported in the subchapter 4.2. The temperature of the reactor has been fixed equal to the experimental one (T = 50 °C). It has been also decided to perform the reaction at high pressure (P = 105 bar), so to enhance the conversion of the CO_2 to the product. Therefore, it has been decided to work at a fixed partial pressure of CO_2 = 60 bar and H_2 = 45 bar, as shown in the green curve of Figure 23b. Considering that the only information related to the catalyst was its molar concentration, it has been decided to not simulate its physical presence in the simulation. Therefore, its effect has been considered in the simulation just by setting its value as a constant in the rate law of the Fortran® subroutine. Considering this assumption, the catalyst separation from the products has not been studied. The reaction occurs in liquid triethylamine and a polar mixture made by water and methanol, and the adduct formed (equation 4.1) should successively be broken into the product and the amine in a reactive distillation. Considering the lack of information to describe this equilibrium at the process pressure, for a simulation purpose, it has been decided to simulate the CSTR with the gas species only, and to add the solvents later, to simulate the separations. It must be noted that for the same lack of information, the adduct of the equation 4.1 which theoretically is formed in the reactor and is subsequently broken (equation 4.2) in a reactive column has not been simulated but, for rigor, it has been added in the solvent stream of triethylamine, the flow of amine necessary to simulate the adduct formation (equation 4.1). In the simulation, however, all the pumps and the heat exchangers and the lamination valves have been included, to have realistic results despite the changing made in the process design. Finally, the separation stages of this simulation have been built according to a patent (Roca and Cited 2006), which implements the experimental information of Jessop et al. (Thomas et al. 2001) in order to build a lab scale complete process. This patent is focused on the study of different amine solvents but, unfortunately it does not study the amine used by the reference article. Considering that the binary parameters of the amines used by the authors was not present in the database, it was decided to maintain the triethylamine and its thermodynamic study developed. The authors purification procedure was anyway considered as a basis for the purification stages of this synthesis.

4.5 Process simulation description

The simulation designed for the synthesis of the formic acid is shown in Figure 25. The process has been designed in order to treat the same flow rate of CO_2 of the Syngas process simulated in the Chapter 3. The CO_2 feed gas (1.5 ton/h), assumed to be available at atmospheric pressure and ambient temperature, is then compressed to the reactor pressure and temperature (P = 105 bar, T = 50 °C) in a multistage compressor (MC1) consisting in four compressor stages with intermediate cooling. The H_2 feed gas follows the same compression stages of the feed CO_2. It should be noted that the amount of H_2 (0.218 ton/h) is determined in order to meet the partial pressures discussed in the subchapter 4.4. The feed gases enter the reactor together with the recycle stream, and the subroutine FORMICAC (Appendix E.1) solves the rate law according to the CSTR reactor balance imposed. The residence time set in the simulation has been chosen as the one reported in the patent of the experiment (1 hour). Therefore, a volume of 30.6 m^3 has resulted necessary to perform the reaction with the recycle, to achieve the required residence time.

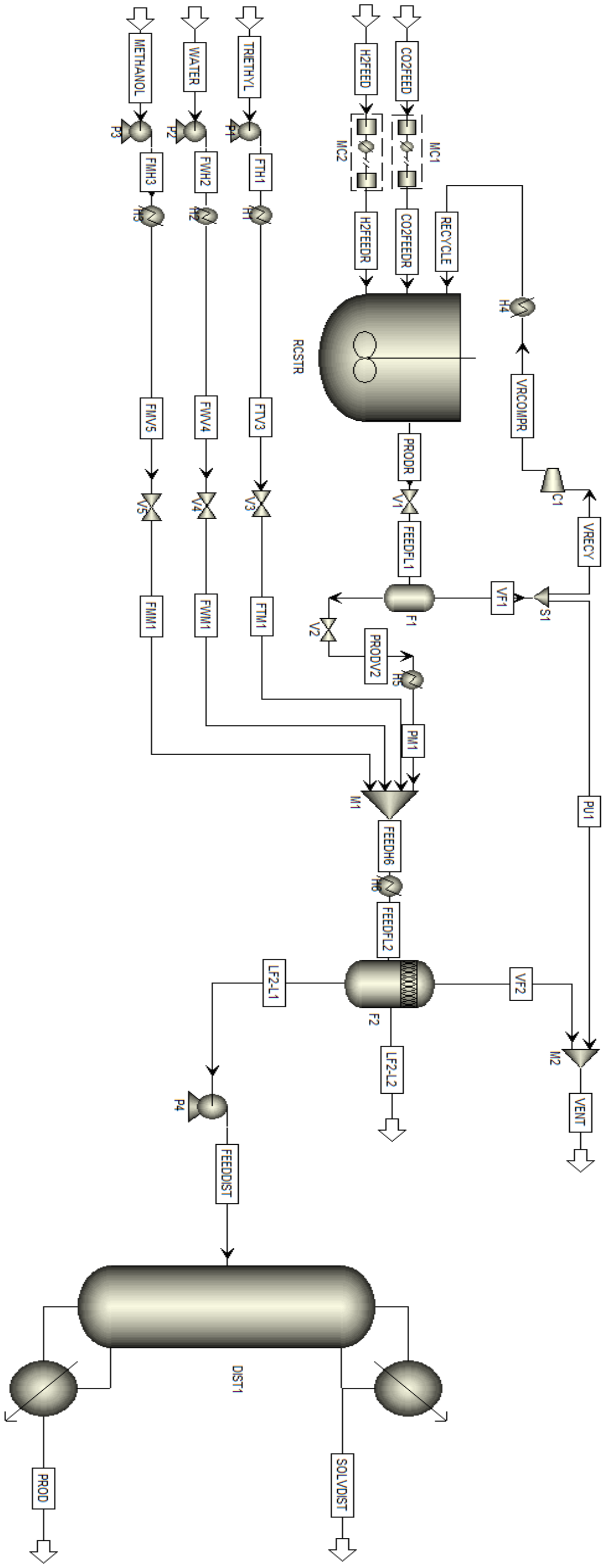

Figure 25: *Flowsheet of the simulated process for the Formic acid synthesis.*

The reactor products stream (PRODR) is then laminated to 70 bar to condense the formic acid and to permit the creation of a biphasic mixture made by the product and the unreacted gases. This mixture is sent to a flash unit working at 70 bar that separates at the top (VF1) the unreacted gases (and a small part of the product), which are recompressed and cooled to the reactor operating conditions. The 5% percent of this stream is purged (PU1) to avoid the mass accumulation. The feed streams of triethylamine (2.317 ton/h), water (0.431 ton/h) and methanol (0.130 ton/h), assumed to be available at atmospheric pressure and ambient temperature, undergo the same compression/heating processes of the feed gases, and then are laminated to the pressure of 1 bar like the liquid bottom stream of the flash F1. All these streams are thus mixed in the mixer M1, in order to reproduce the patent mixture entering the liquid-liquid separation. At this point, it is introduced the separation of the polar solvent from the amine adduct at 50°C as reported from the patent. This has been done through the Vapour-Liquid-Liquid (VLL) flash (F2), which through a rigorous calculation, allows to separate the remaining unreacted gas from the top, the polar mixture (LF2-L2) from a side, and the adduct rich in amine in the other. Unfortunately, half of the water and a good part of the methanol exit from the flash stage into the adduct stream. Such a mixture is characterized by an equilibrium that involves the formation of azeotropes that make it non-trivial to separate the product of interest. It has been tried to replicate the 3 bar distillation separation of the products in the column DIST1, but this results in an extraction from the bottom product of the column of the Formic acid-triethylamine azeotrope (70 wt% at T = 174 °C) and not, of the pure product (T = 100.8 °C). The possibility of finding a proper solvent (e.g. dimethylformamide) to carry out the separation of these two components by means of extractive distillation was investigated, but no solvent was found effective in this regard. This suggests that a different amine, with higher boiling point and not forming azeotropes with formic acid, should be investigated for this process.

4.6 Simulation results and discussion

The results obtained from the process simulation are summarized in Table 16 and are written in the form of the technological parameters needed for the final processes comparisons (for the derivation, see Appendix E.2).

Table 16: *Results obtained from the formic acid synthesis process simulation.*

$\Delta CO_2/CO_{2,in}$	$H_2O/CO_{2,in}$	$H_2/CO_{2,in}$	Therm.en.cons./$CO_{2,in}$	Electr.cons./$CO_{2,in}$
[-]	**ton H_2O/ton $CO_{2,in}$**	**ton H_2/ton $CO_{2,in}$**	**MW_h/ton $CO_{2,in}$**	**MW_h/ton $CO_{2,in}$**
0.957	0	0.146	1.236*	0.176*

The thermal energy consumption and the electricity consumption marked with an asterisk, because the simulation has been stopped at the distillation stage and therefore, the energy required to separate the product and recycle the solvents has not been considered. However, considering the complexity of this synthesis and the rigorous work done with the reactor, this simulation can be considered a good starting point that can be concluded once an intense thermodynamic study of this process will be developed by some research team interested in the CO_2 hydrogenation to formic acid process.

4.7 Final comparison of the five processes

In Table 17 are summarized all the results obtained for the five different hydrogenation processes investigated. The results in bold, represent the best values for that parameter among the different investigated processes.

Table 17: *Summary of the simulation results. The results in bold, represent the best value for that parameter.*

Process	ΔCO/ CO_2,in	H_2O/ CO_2,in	H_2/ CO_2,in	Therm.en.cons./ CO_2,in	Electr.cons./ CO_2,in
	[-]	ton H_2O/ ton CO_2,in	ton H_2/ ton CO_2,in	MW_h/ ton CO_2,in	MW_h/ ton CO_2,in
Methanol	0.938	0.390	**0.136**	0.891	**0.116**
Methane	0.985	0.801	0.183	**0.595**	0.122
Urea	0.996	0.412	0.137	4.571	0.955
Syngas	**0.997**	0.408	0.162	0.787	0.430
Formic acid	0.957	**0**	0.146	1.236*	0.176*

Conclusions

Among the different solutions for the CO_2 reduction, the hydrogenation of the CO_2 could become a new class of sustainable processes for the transformation of the CO_2 from a waste and pollutant material to a series of new chemicals that can be used in a wide variety of industrial sectors. In this thesis, five different processes of CO_2 hydrogenation have been investigated: the methanol synthesis, the methane synthesis, the urea synthesis, the syngas synthesis and the formic acid synthesis. The main limitation found in this study was the lack of scientific information or sometimes, the ambiguity of the results reported by the authors. Through a deep research of process information and data analysis it has been possible to simulate two processes and investigate other three from the scientific literature. The final objective of this research was therefore the comparison of this five hydrogenation processes through five technological parameters. The first technological parameter, the CO_2 conversion, is characterised by very high values, where, the syngas synthesis, with a value of 99.7% has resulted the highest value. From the second technological parameter, the specific water production (with respect to the CO_2 treated in the process), it has derived that the methane process, with a value of 0.801 $tonH_2O/tonCO_2$, was the hydrogenation process with the highest production of water per tonne of CO_2 treated therefore, the process that waste more hydrogen to produce the unwanted product while, the formic acid synthesis does not produce water. The third technological parameter, the hydrogen requirement per CO_2 treated in the process, is the parameter that has been resulted the most regular between the five processes, ranging in the interval [0.136; 0.183] $tonH_2/tonCO_2$, with the methane synthesis requiring the highest amount. The fourth technological parameter, the specific thermal energy consumption, has resulted as the parameter with the highest variability with respect to the others. Considering that in the urea synthesis it has been considered the thermal energy required to produce the ammonia necessary for the urea synthesis, this hydrogenation process has resulted the one with the highest thermal energy requirement, with a value of 4.571 $MW_h/tonCO_2$. On the other hand, the methane synthesis has resulted the synthesis with the lowest energy requirement, with a value of 0.595 $MW_h/tonCO_2$. The last technological parameter, the specific electricity, shows, for the same reasons of the previous one, that the urea synthesis is the process with the highest electricity requirement per tonne of CO_2 treated, with a value of 0.955 $MW_h/tonCO_2$, while the methanol synthesis has resulted the synthesis with the lowest electricity requirement, with a value of 0.116 $MW_h/tonCO_2$. Considering the results obtained, it can be concluded that the hydrogenation processes of the CO_2 could become a part of the modern industrial processes and therefore, the research and the process design of these synthesis could be considered as means to mitigate the CO_2 impact.

Appendix A

Appendix A reports the derivation of the technological parameters for the methanol synthesis. The parameters are calculated in the following equations:

$$\frac{\Delta CO_2}{CO_2\ in} = 0.938 \tag{A.1}$$

$$\frac{H_2O}{CO_2 in} = \frac{0.569\,\frac{ton\ H_2O}{ton\ MeOH}}{1.460\,\frac{ton\ CO_2 in}{ton\ MeOH}} = 0.390\,\frac{ton\ H_2O}{ton\ CO_2 in} \tag{A.2}$$

$$\frac{H_2}{CO_2 in} = \frac{0.199\,\frac{ton\ H_2}{ton\ MeOH}}{1.460\,\frac{ton\ CO_2 in}{ton\ MeOH}} = 0.136\ \frac{ton\ H_2}{ton\ CO_2 in} \tag{A.3}$$

$$\frac{Therm.en.cons.}{CO_2 in} = \frac{1.301\,\frac{MW}{ton\ MeOH}}{1.460\ \frac{ton\ CO_2 in}{ton\ MeOH}} = 0.891\ \frac{MW_h}{ton\ CO_2 in} \tag{A.4}$$

$$\frac{Electr.cons.}{CO_2 in} = \frac{0.169\,\frac{MW}{ton\ MeOH}}{1.460\,\frac{ton\ CO_2 in}{ton\ MeOH}} = 0.116\ \frac{MW_h}{ton\ CO_2 in} \tag{A.5}$$

Appendix B

Appendix B contains the flowsheet of the reference simulation for the methane process and the technological parameters calculation for this synthesis.

B.1 Flowsheet of the reference simulation for the methane process

Figure B1 shows the flowsheet of the complete methane process simulation developed by the authors (De Saint Jean, Baurens, and Bouallou 2014).

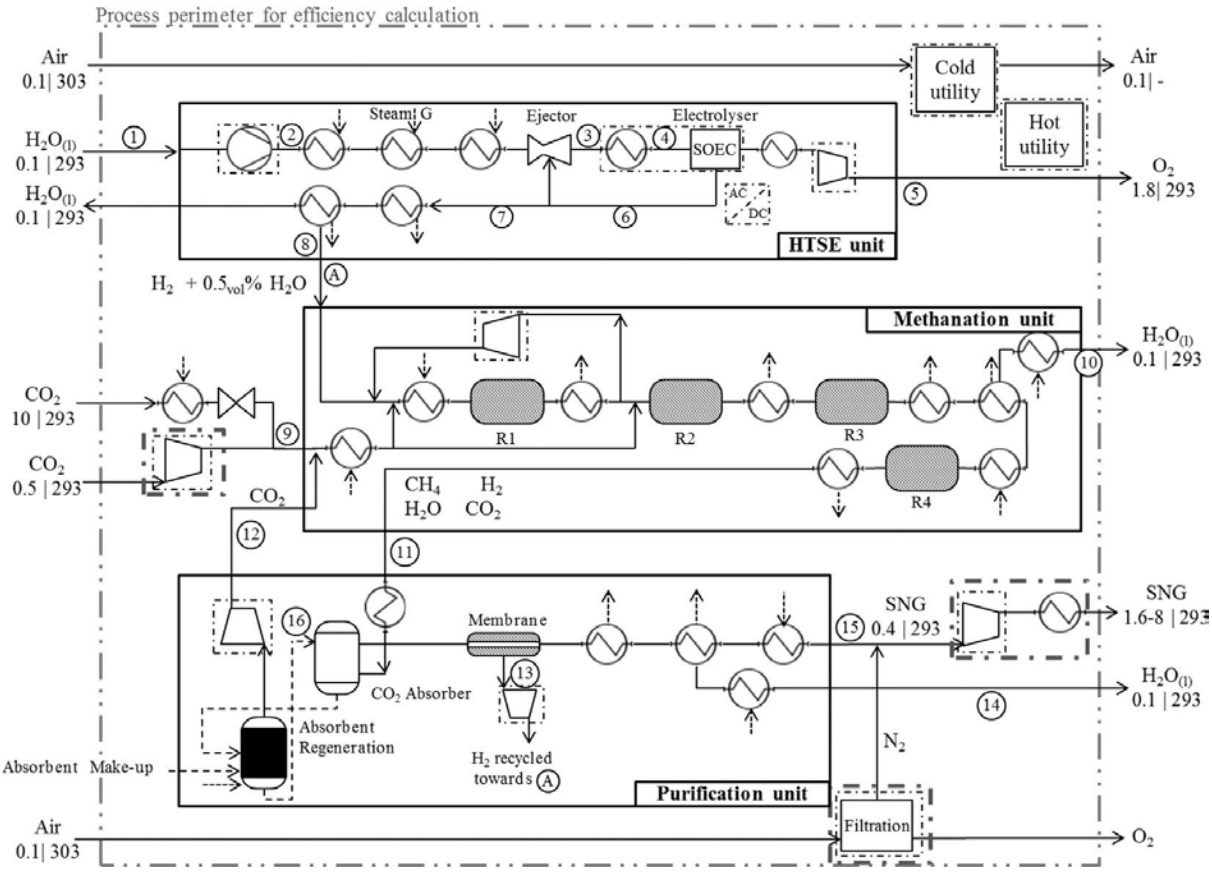

Figure B1: *Flowsheet of the complete methane process simulation.*

B.2 Technological parameters calculation for the methane process

It is reported the derivation of the technological parameters for the methane synthesis where, in the equations: B.1, B.2, B.3 and B.4; the streams results obtained by the authors are first converted from Nm^3/h to ton/h and, in the equations B.5 and B.6 are reported the total thermal and electrical energy consumption estimated.

$$CO_2\ in = (N_2) + (N_5 * 0.986) =$$
$$= 66.4\ \frac{Nm^3}{h}[303\ K\ ; 0.74\ MPa] + 0.296\ \frac{Nm^3}{h}[476\ K\ ; 0.78\ MPa] =$$
$$= 2.962\ \frac{kmol}{h} + 0.013\ \frac{kmol}{h} = 130.376\ \frac{kg}{h} + 0.581\ \frac{kg}{h} = 0.131\ \frac{ton\ CO_2\ in}{h} \tag{B.1}$$

$$CO_2\ out = (N_4 * 0.017) = 1.321\ \frac{Nm^3}{h}[293\ K\ ; 0.44\ MPa] =$$
$$= 0.059\ \frac{kmol}{h} = 2.594\ \frac{kg}{h} = 0.002\ \frac{ton\ CO_2\ out}{h} \tag{B.2}$$

$$H_2\ in = (N_1 * 0.995) + (N_5 * 0.0002) =$$
$$= 262.481\ \frac{Nm^3}{h}[301\ K\ ; 0.74\ MPa] + 0.00006\frac{Nm^3}{h}[476\ K\ ; 0.78\ MPa] =$$
$$= 11.711\ \frac{kmol}{h} + 2.677\ e^{-6}\ \frac{kmol}{h} = 23.607\ \frac{kg}{h} + 5.396\ e^{-6}\ \frac{kg}{h} = 0.024\ \frac{ton\ H_2\ in}{h} \tag{B.3}$$

$$H_2O\ out = (N_3) + (N_4 * 0.072) - (N_1 * 0.005) - (N_5 * 0.01) =$$
$$= 126.4\ \frac{Nm^3}{h}[293\ K\ ; 0.1\ MPa] + 5.594\ \frac{Nm^3}{h}[293\ K\ ; 0.44\ MPa] +$$
$$- 1.319\ \frac{Nm^3}{h}[301\ K\ ; 0.74\ MPa] - 0.003\ \frac{Nm^3}{h}[476\ K\ ; 0.78\ MPa] =$$
$$= 5.639\ \frac{kmol}{h} + 0.250\ \frac{kmol}{h} - 0.059\ \frac{kmol}{h} - 1.338\ e^{-4}\frac{kmol}{h} =$$
$$= 101.594\ \frac{kg}{h} + 4.496\ \frac{kg}{h} - 1.060\ \frac{kg}{h} - 0.002\ \frac{kg}{h} =$$
$$= 0.105\ \frac{ton\ H_2O\ out}{h} \tag{B.4}$$

$$Thermal\ energy\ consumption = 0.078\ MW \tag{B.5}$$

$$Electricity\ consumption = 0.016\ MW \tag{B.6}$$

In the equations: B.7, B.8, B.9, B.10, B.11; are therefore calculated the technological parameters for the methane synthesis.

$$\frac{\Delta CO_2}{CO_2 in} = \frac{(0.131 - 0.002)\frac{ton}{h}}{0.131\,\frac{ton\ CO_2\ in}{h}} = 0.985 \tag{B.7}$$

$$\frac{H_2O\ out}{CO_2 in} = \frac{0.105\,\frac{ton\ H_2O\ out}{h}}{0.131\,\frac{ton\ CO_2\ in}{h}} = 0.801\ \frac{ton\ H_2O\ out}{ton\ CO_2\ in} \tag{B.8}$$

$$\frac{H_2\ in}{CO_2 in} = \frac{0.024\,\frac{ton\ H_2\ in}{h}}{0.131\,\frac{ton\ CO_2\ in}{h}} = 0.183\ \frac{ton\ H_2\ in}{ton\ CO_2\ in} \tag{B.9}$$

$$\frac{Therm.en.cons.}{CO_2 in} = \frac{0.078\ MW}{0.131\,\frac{ton\ CO_2\ in}{h}} = 0.595\ \frac{MW_h}{ton\ CO_2 in} \tag{B.10}$$

$$\frac{Electr.cons.}{CO_2 in} = \frac{0.016\ MW}{0.131\,\frac{ton\ CO_2\ in}{h}} = 0.122\ \frac{MW_h}{ton\ CO_2 in} \tag{C.11}$$

Appendix C

Appendix C reports the derivation of the technological parameters for the urea synthesis. As the process simulation considered takes into account the reaction of CO_2 with NH_3, in order to obtain the corresponding hydrogen consumption of the urea synthesis, the hydrogen necessary to produce the ammonia feed required for the urea synthesis was evaluated. The reference process is the well known Haber-Bosch. Accordingly, it has been taken into account also the thermal and electrical consumption necessary to produce the ammonia feed required for the synthesis. The results of these calculations are reported in the following equations.

$$\frac{H_2\ used}{NH_3\ produced} = \frac{4\,872.020\,\frac{kmol\,H_2}{h}}{3\,247.942\,\frac{kmol\,NH_3}{h}} = 1.500\ \frac{kmol\ H_2}{kmol\ NH_3} = \frac{9.792\,\frac{ton\,H_2}{h}}{55.315\,\frac{ton\,NH_3}{h}} = 0.177\ \frac{ton\ H_2 used}{ton\ NH_3} \tag{C.1}$$

$$Therm.en.cons.^{Ammonia} = 104.347\ MW \tag{C.2}$$

$$Electr.cons.^{Ammonia} = 22.389\ MW \tag{C.3}$$

The results obtained from the urea simulation are reported in the following equations:

$$CO_2\ in = 711.500\ \frac{kmol}{h} = 31.313\ \frac{ton\ CO_2\ in}{h} \tag{C.4}$$

$$NH_3\ in = 1\,418.250\ \frac{kmol}{h} = 24.153\ \frac{ton\ NH_3\ in}{h} \tag{C.5}$$

$$Urea\ out = 708.870\ \frac{kmol}{h} = 42.571\ \frac{ton\ Urea\ out}{h} \tag{C.6}$$

$$CO_2\ out = 2.589\ \frac{kmol}{h} = 0.114\ \frac{ton\ CO_2\ out}{h} \tag{C.7}$$

$$H_2O\ out = 0.211\ \frac{kmol}{h} + 716.579\ \frac{kmol}{h} = 716.790\ \frac{kmol}{h} = 12.913\ \frac{ton\ H_2O\ out}{h} \tag{C.8}$$

$$Therm.en.cons.^{Urea} = 38.800\ MW \tag{C.9}$$

$$Electr.cons.^{Urea} = 7.296\ MW \tag{C.10}$$

Finally, the technological parameters for the urea synthesis are derived as in the following equations:

$$\frac{\Delta CO_2}{CO_2 in} = 0.996 \tag{C.11}$$

$$\frac{H_2O}{CO_2 in} = 0.412\ \frac{ton\ H_2O}{ton\ CO_2 in} \tag{C.12}$$

$$\frac{H_2^{Urea}}{CO_2 in}\ (mass) = \frac{4.276\ \frac{ton\ H_2}{h}}{31.313\ \frac{ton\ CO_2 in}{h}} = 0.137\ \frac{ton\ H_2}{ton\ CO_2 in} \tag{C.13}$$

$$\frac{Therm.en.cons.}{CO_2 in} = \frac{Therm.en.cons.^{Ammonia} + Therm.en.cons.^{Urea}}{31.313\ \frac{ton\ CO_2 in}{h}} = \frac{(38.800 + 104.347)\ MW}{31.313\ \frac{ton\ CO_2 in}{h}}$$

$$= \frac{(38.800 + 104.347)\ MW}{31.313\ \frac{ton\ CO_2 in}{h}} = 4.571\frac{MW_h}{ton\ CO_2 in} \tag{C.14}$$

$$\frac{Electr.cons.}{CO_2 in} = \frac{Electr.cons.^{Ammonia} + Electr.cons.^{Urea}}{CO_2 in} = \frac{(7.296 + 22.389)\ MW}{31.313\ \frac{ton\ CO_2 in}{h}} = 0.955\ \frac{MW_h}{ton\ CO_2 in} \tag{C.15}$$

Appendix D

Appendix D contains the Fortran® code applied in the calculator of the syngas process simulation and the technological parameters calculation for this synthesis.

D.1 Calculator code for the syngas process simulation

Fortran® code applied to the syngas simulation calculator to predict the outputs of the reactor.

```
c
c  Program for the product prediction
c
c  datas: average + st.deviation of 1 = CO2, 2 = H2, 3 = T, 4 = t
c

   aver1 = 29.45
   stdev1 = 10.29535263

   aver2 = 70.55
   stdev2 = 10.29535263

   aver3 = 613.75
   stdev3 = 63.00510183

   aver4 = 142.5
   stdev4 = 139.5656528

c  normalized value for yi calculation OBS: time r manually insert

    o = (FEEDCO2 - aver1)/(stdev1)
    p = (FEEDH2 - aver2)/(stdev2)
    q = (T - aver3)/(stdev3)
    r = (60 - aver4)/(stdev4)

c  coefficient values from the PLS regression
```

```
      a=0.3390
      b=0.3390
      c=0.2918
      d=0.1115
      e=0.3458
      f=0.3458
      g=0.2976
      h=0.1137
      i=0.3247
      l=0.3247
      m=0.2794
      n=0.1068

c     yi calculating

      CO2CALC=a*o-b*p+c*q-d*r

      H2CALC=-e*o+f*p-g*q+h*r

      COCALC=i*o-l*p+m*q-n*r

c     aver. + st.dev datas for the output predictions: 11 =CO2 , 22 =H2 , 33 =CO

      aver11 =18.8625
      stdev11 =9.628074648

      aver22 =66.275
      stdev22 =12.60405

      aver33 =14.95
      stdev33 =3.742421

c     output predictions

     CO2OUT=CO2CALC*stdev11 +aver11
     H2OUT=H2CALC*stdev22 +aver22
     COOUT=COCALC*stdev33 +aver33
```

```
      H2OOUT=COOUT

c  output moles sum for the normalization

      sum=CO2OUT+H2OUT+COOUT+H2OOUT

c  moles obtained after the reactor before the trap

      CO2PROD=(CO2OUT/sum)*100
      H2PROD=(H2OUT/sum)*100
      COPROD=(COOUT/sum)*100
      H2OPROD=(H2OOUT/sum)*100

c  conversion calculation

      XCO2=(FEEDCO2-CO2PROD)/(FEEDCO2)
```

D.2 Technological parameters calculation for the syngas process

It is reported the derivation of the technological parameters for the syngas synthesis simulated. The parameters are calculated in the following equations:

$$\frac{\Delta CO_2}{CO_2 in} = \frac{(\,1.493 - 0.004\,)\,\frac{ton}{h}}{1.493\ \frac{ton}{h}} = 0.997 \tag{D.1}$$

$$\frac{H_2O}{CO_2 in} = \frac{0.609\,\frac{ton}{h}}{1.493\,\frac{ton}{h}} = 0.408\ \frac{ton\ H_2O}{ton\ CO_2 in} \tag{D.2}$$

$$\frac{H_2}{CO_2 in} = \frac{0.242\,\frac{ton\ H_2}{h}}{1.493\,\frac{ton\ CO_2 in}{h}} = 0.162\ \frac{ton\ H_2}{ton\ CO_2 in} \tag{D.3}$$

$$\frac{Therm.en.cons.}{CO_2 in} = \frac{1.181\ MW}{1.493\,\frac{ton}{h}} = 0.787\ \frac{MW_h}{ton\ CO_2 in} \tag{D.4}$$

$$\frac{Electr.cons.}{CO_2 in} = \frac{0.643\ MW}{1.493\,\frac{ton}{h}} = 0.430\ \frac{MW_h}{ton\ CO_2 in} \tag{D.5}$$

Appendix E

Appendix E contains the Fortran® subroutine applied to the formic acid process simulation and the technological parameters calculation for this synthesis.

E.1 Subroutine used for the formic acid process simulation

It is reported the Fortran® FORMICAC subroutine used in the formic acid simulation to solve the reactor balance.

```
C$ #2 BY: PATNAIK DATE: 14-NOV-1998 INCLUDE COMMONS FOR RADFRAC/RATEFRAC
C$ #1 BY: ANAVI DATE:  1-JUL-1994 NEW FOR USER MODELS
C
C      User Kinetics Subroutine for RCSTR, RPLUG, RBATCH, PRES-RELIEF,
C      RADFRAC and RATEFRAC (USER type Reactions)
C
      SUBROUTINE FORMICAC   (SOUT,    NSUBS,   IDXSUB,   ITYPE,   NINT,
     2                   INT,     NREAL,   REAL,     IDS,     NPO,
     3                   NBOPST, NIWORK, IWORK,     NWORK,   WORK,
     4                   NC,      NR,      STOIC,    RATES,   FLUXM,
     5                   FLUXS,  XCURR,   NTCAT,    RATCAT, NTSSAT,
     6                   RATSSA, KCALL,   KFAIL,    KFLASH, NCOMP,
     7                   IDX,     Y,       X,        X1,      X2,
     8                   NRALL,  RATALL, NUSERV,   USERV,   NINTR,
     9                   INTR,    NREALR, REALR,    NIWR,    IWR,
     *                   NWR,     WR,      NRL,      RATEL,   NRV,
     1                   RATEV)
C
      IMPLICIT NONE
C
C      DECLARE VARIABLES USED IN DIMENSIONING
C
      INTEGER NSUBS, NINT,  NPO,   NIWORK,NWORK,
     +        NC,    NR,    NTCAT, NTSSAT,NCOMP,
     +        NRALL, NUSERV,NINTR, NREALR,NIWR,
     +        NWR

C     conveniently stores run time control flags
#include "ppexec_user.cmn"

C     default values for real parameter  ,  default values for integer parameter

C       EQUIVALENCE (RMISS, USER_RUMISS)
C     EQUIVALENCE (IMISS, USER_IUMISS)

C     contains component-related stream segment
#       INCLUDE "dms_ncomp.cmn"
C
C      Reaction considered : CO2 + H2 = HCOOH
C
C.....RCSTR......
C     contains integer parameter config for the block
```

```
c     include "rcst_rcstri.cmn"
C
C     contains real parameter config for the block
#       include "rxn_rcstrr.cmn"
C     RCSTR reactor volume
        EQUIVALENCE (VOL, RCSTRR_VOLRC)

C
C.....RPLUG...
c include "rplg_rplugi.cmn"
C       include "rplg_rplugr.cmn"
C      EQUIVALENCE (XLEN, RPLUGR_UXLONG)
C      EQUIVALENCE (DIAM, RPLUGR_UDIAM)
C
C.....RBATCH...
cinclude "rbtc_rbati.cmn"
cinclude "rbtc_rbatr.cmn"
C
C.....PRES-RELIEF...
cinclude "prsr_presri.cmn"
cinclude "rbtc_presrr.cmn"
C
C.....RADFRAC/RATEFRAC
cinclude "rxn_disti.cmn"
cinclude "rxn_distr.cmn"
C
C.....REACTOR (OR PRES-RELIEF VESSEL OR STAGE) PROPERTIES...
C
C     contains real property values, such as temperature and pressure, for the reaction
calculations
#       include "rxn_rprops.cmn"

C     Reactor/stage temperature (K)
       EQUIVALENCE (TEMP, RPROPS_UTEMP)
C     Reactor/stage pressure (N/m^2)
       EQUIVALENCE (PRES, RPROPS_UPRES)
C     Molar vapor fraction in the reactor/stage
       EQUIVALENCE (VFRAC, RPROPS_UVFRAC)
C     Liquid 1/Total liquid molar ratio in the reactor/stage
       EQUIVALENCE (BETA, RPROPS_UBETA)
C     Volume occupied by the vapor phase in the reactor (m^3)
       EQUIVALENCE (VVAP, RPROPS_UVVAP)
C     Volume occupied by the liquid phase in the reactor (m^3)
       EQUIVALENCE (VLIQ, RPROPS_UVLIQ)

C     contains indexes and dimension for the stream flash work area
#       include "shs_stwork.cmn"
C
C      INITIALIZE RATES
C
C
C      DECLARE ARGUMENTS
C
       INTEGER IDXSUB(NSUBS),ITYPE(NSUBS), INT(NINT),
     +         IDS(2),NBOPST(6,NPO),IWORK(NIWORK),
     +         IDX(NCOMP),   INTR(NINTR),   IWR(NIWR),
     +         NREAL, KCALL, KFAIL, KFLASH,NRL,
     +         NRV,    I
       REAL*8  SOUT(1),       WORK(NWORK),
     +         STOIC(NC,NSUBS,NR),  RATES(1),
     +         FLUXM(1),     FLUXS(1),     RATCAT(NTCAT),
```

```
     +        RATSSA(NTSSAT),      Y(NCOMP),
     +        X(NCOMP),     X1(NCOMP),    X2(NCOMP)
      REAL*8  RATALL(NRALL), USERV(NUSERV),
     +        REALR(NREALR), WR(NWR),      RATEL(1),
     +        RATEV(1),  XCURR, k2,  k4,  corr,  cat,  vol,
     +        P1, P2, k22, k44


C
C     DECLARE LOCAL VARIABLES
C
      INTEGER IMISS
      REAL*8 REAL(NREAL),  RMISS, XLEN,  DIAM,  TEMP,
     +       PRES,  VFRAC, BETA,  VVAP,  VLIQ,
     +       VLIQS, PRESS, M(6), R, RC, V, N(6), L(6), tau(1), PREACT,
     +       MM(2), MN(2), TOFc, TOF, VV, VL, G, VR, tauv, taul

C
C     BEGIN EXECUTABLE CODE
C
C     Kinetic constants estrapolated from the article (with the model correction)
[1/s/bar]
C
      k2 = 0.00001376208
      k4 = 0.01942411111

C     Kinetic constants estrapolated from the article (with the model correction) for
TOF calc   [1/h/bar]

      k22 = 0.0495435
      k44 = 69.9268

C     corr: model correction factor    [1/bar]

      corr = 0.0145095

C     Molar concentration of the Rutot catalist    [kmol/m^3]

      cat = 0.000096774

C     Reactor volume [m^3]

      VR = VVAP + VLIQ

C     Total molar flow rate  [kmol/s]  ,  Number of conventional components defined by
user + components generated

       M(1) = SOUT(NCOMP_NCC+1)

C     Total molar flow rate in vapor phase  [kmol/s]

       MM(1) = M(1)*(VFRAC)

C     Total molar flow rate in liquid phase  [kmol/s]

       MN(1) = M(1)*(1 - VFRAC)

C     Vapor volume [m^3/kmol]

      VV = stwork_vv
```

```
C      Liquid volume [m^3/kmol]

       VL = stwork_vl

C      Volumetric flow rate calculated in V  [m^3/s]

       V = MM(1)*VV

C      Volumetric flow rate calculated in L  [m^3/s]

       G = MN(1)*VL

C      Molar flow rate in V PROD    1 = H2  ,  2 = CO2  ,  3 = HCOOH     [kmol/s]

       N(1) = MM(1)*Y(1)
       N(2) = MM(1)*Y(2)
       N(3) = MM(1)*Y(3)

C      Molar flow rate in L PROD    1 = H2  ,  2 = CO2  ,  3 = HCOOH     [kmol/s]

       L(1) = MN(1)*X(1)
       L(2) = MN(1)*X(2)
       L(3) = MN(1)*X(3)

C      Reactor residence time calculation  [s]

       tau(1) = (VVAP + VLIQ)/(V + G)

C      Reactor Vapor residence time calculation  [s]

       tauv = VVAP/V

C      Reactor Liquid residence time calculation  [s]

       taul = VLIQ/G

C      Reactor pressure conversion [Pa] to [bar]

       PREACT = PRES*0.00001

C      Partial pressure pi of the two reagents unreacted:    1 = H2  and  2 = CO2
[bar]  Ptot = 105 bar

       P1 = PREACT*Y(1)
       P2 = PREACT*Y(2)

C      reaction Rates R without correction for the TOF calculation  [kmol/s/m^3]

       R = ((k2*k4*P1*P2)/((1 + k2*P2)/3600))*cat

C      reaction Ratetes Corrected RC [kmol/s/m^3]  ; (denominator in sec) ; (Model
corrected)

       RC = ((k2*k4*P1*P2)/((1 + (k2*P2)**(corr*P1))/3600))*cat

C      Reaction rates calculation [kmol/s]

       RATES(1) = -1*RC*(VVAP)                       ! H2
       RATES(2) = -1*RC*(VVAP)                       ! CO2
       RATES(3) = 1*RC*(VVAP)                        ! HCOOH
```

```
C     Turnover frequency with the model correction  [1/h]

      TOFc = ((k22*k44*P1*P2)/(1 + (k22*P2)**((corr*P1)/3600)))

C     Turnover frequency  [1/h]

      TOF = ((k22*k44*P1*P2)/(1 + k22*P2))



      open(1,FILE='cstrformic.dat')

      write (1, *) k2*3600, 'k2 value [1/h/bar]'
      write (1, *) k4*3600, 'k4 value [1/h/bar]'
      write (1, *) corr, 'n correction value [1/bar]'

      write (1, *) VR, 'V CSTR Reactor [m^3]'
      write (1, *) VVAP, 'V occup. by the vap. phase in the react.[m^3]'
      write (1, *) VLIQ, 'V occup. by the liq. phase in the react.[m^3]'
      write (1, *) VV, 'Vapor volume [m^3/kmol]'
       write (1, *) V*3600, 'Volumetric flow rate in V [m^3/h]'
      write (1, *) VL, 'Liquid volume [m^3/kmol]'
      write (1, *) G*3600, 'Volumetric flow rate in L [m^3/h]'

      write (1, *) tau(1)/3600, 'Ractor residence time [h]'
      write (1, *) tauv/3600, 'Ractor V residence time [h]'
      write (1, *) taul/3600, 'Ractor L residence time [h]'

      write (1, *) M(1)*3600, 'Total molar flow rate [kmol/h]'
      write (1, *) MM(1)*3600, 'Tot molar flow rate in V phase [kmol/h]'
      write (1, *) MN(1)*3600, 'Tot molar flow rate in L phase [kmol/h]'

      write (1, *) PREACT, 'Reactor pressure [bar]'
      write (1, *) P1, 'Partial pressure of H2 [bar]'
      write (1, *) P2, 'Partial pressure of CO2 [bar]'

      write (1, *) Y(1), 'H2 vapor fraction in the PROD [-]'
      write (1, *) Y(2), 'CO2 vapor fraction in the PROD [-]'
      write (1, *) Y(3), 'HCOOH vapor fraction in the PROD [-]'

      write (1, *) N(1)*3600, 'H2 molar flow rate in V [kmol/h]'
      write (1, *) N(2)*3600, 'CO2 molar flow rate in V [kmol/h]'
      write (1, *) N(3)*3600, 'HCOOH molar flow rate in V [kmol/h]'

      write (1, *) X(1), 'H2 liquid fraction in the PROD [-]'
      write (1, *) X(2), 'CO2 liquid fraction in the PROD [-]'
      write (1, *) X(3), 'HCOOH liquid fraction in the PROD [-]'

      write (1, *) L(1)*3600, 'H2 molar flow rate in L [kmol/h]'
      write (1, *) L(2)*3600, 'CO2 molar flow rate in L [kmol/h]'
      write (1, *) L(3)*3600, 'HCOOH molar flow rate in L [kmol/h]'

      write (1, *) RC, 'Reaction rate [kmol/s/m^3] (kin. model correc.)'
      write (1, *) R, 'Reaction rate [kmol/s/m^3]'
      write (1, *) RATES(3), 'HCOOH rates [kmol/s]'

      write (1, *) TOFc, 'TOFc with model correction [1/h]'
      write (1, *) TOF, 'TOF [1/h]'
```

```
 close(1,STATUS='keep')

RETURN
END
```

E.2 Technological parameters calculation for the formic acid process

It is reported the derivation of the technological parameters for the formic acid synthesis simulated. The parameters are calculated in the following equations:

$$\frac{\Delta CO_2}{CO_2 in} = \frac{(1.493-0.064)\frac{ton}{h}}{1.493\frac{ton}{h}} = 0.957 \tag{E.1}$$

$$\frac{H_2O}{CO_2 in} = 0\ \frac{ton\ H_2O}{ton\ CO_2 in} \tag{E.2}$$

$$\frac{H_2}{CO_2 in} = \frac{0.218\frac{ton\ H_2}{h}}{1.493\frac{ton\ CO_2 in}{h}} = 0.146\ \frac{ton\ H_2}{ton\ CO_2 in} \tag{E.3}$$

$$\frac{Therm.en.cons.}{CO_2 in} = \frac{1.845\ MW}{1.493\frac{ton\ CO_2 in}{h}} = 1.236\ \frac{MW_h}{ton\ CO_2 in} \tag{E.4}$$

$$\frac{Electr.cons.}{CO_2 in} = \frac{0.263\ MW}{1.493\frac{ton\ CO_2 in}{h}} = 0.176\ \frac{MW_h}{ton\ CO_2 in} \tag{E.5}$$

References

Ampelli, C., Perathoner, S., Centi, G. (2015). “CO_2 Utilization: An Enabling Element to Move to a Resource-and Energy-Efficient Chemical and Fuel Production.” *Philosophical Transactions of the Royal Society A: Mathematical, Physical and Engineering Sciences,* **72**, *1-154.*

Barker, M., Rayens, W. (2003). “Partial Least Squares for Discrimination.” *Journal of Chemometrics*, **17**, 166-173.

Bussche, K.M., Froment, G.F. (1996). “A Steady-State Kinetic Model for Methanol Synthesis and the Water Gas Shift Reaction on a Commercial Cu/ZnO/Al_2O_3 Catalyst.” *Journal of Catalysis*, **161**, 1-10.

Centi, G., Perathoner, S. (2009). “Opportunities and Prospects in the Chemical Recycling of Carbon Dioxide to Fuels.” *Catalysis Today*, **148** (3), 191-201.

Cowin, P. I., Petit, T.G., Rong, L., Irvine, J., Tao, S. (2011). “Recent Progress in the Development of Anode Materials for Solid Oxide Fuel Cells.” *Advanced Energy Materials*, **1**, 314-332.

European Commission (EU). 2012. Commision staff working paper “Communication from the commision to the council, the european parliament, the european economic and social committee and the regions.” *Policy*, 1–24. Brussels (EU)

Gerda, G. (2013). “Hydrogen from Renewable Electricity: An International Review of Power-to-Gas Pilot Plants for Stationary Applications.” *International Journal of Hydrogen Energy,* **38**, 2039-2061.

Gao, J., Wang, Y., Ping, Y., Hu, D., Xu, G., Gu, F., Su, F. (2012). “A Thermodynamic Analysis of Methanation Reactions of Carbon Oxides for the Production of Synthetic Natural Gas.” *RSC Advances*, **2**, 2358-2368.

Graaf, G. H., Sijtsema, P., Stamhuis, E. J., Joosten, G. (1986). “Chemical Equilibria in Methanol Synthesis.” *Chemical Engineering Science*, **41**, 2883-2890.

Hernandez, M. A., Torero, M. (2010). “Fertilizer Market Situation: Market Structure, Consumption and Trade Patterns, and Pricing Behavior.” *International Food Policy Reserach Institute*, 3-72.

Homs, N., Toyir, J., De la Piscina, P.R. (2013). Chapter 1 - Catalytic Processes for Activation of CO2, Suib, Steven L, New and Future Developments in Catalysis, Elsevier, 1-26, Amsterdam.

Hu, B., Guild, C., Suib, S. L. (2013). “Thermal, Electrochemical, and Photochemical Conversion of CO_2 to Fuels and Value-Added Products.” *Journal of CO2 Utilization*, **1**, 18-27.

Hunt, A. J., Sin, E., Marriott, R., Clark, J. H. (2010). "Generation, Capture, and Utilization of Industrial Carbon Dioxide." *ChemSusChem,* **3**, 306-322.

IEA (2015). "Total Greenhouse Gas Emission." *CO_2 EMISSIONS FROM FUEL COMBUSTION (2015 Edition)*, 1–43.

IPCC (2014). "5th Assessment Report: Summary for Policymakers." *IPCC Fifth Asessement Report: Working Group III Mitigation of Climate Change*.

Kusuo N., Sekiya, M. (1977) "Vapor-Liquid Equilibrium for Formic Acid-Triethylamine System Examined by the Use of a Modified Still. Formic Acid-Trialkylamine Azeotropes". *Journal of CO2 Utilization*, **25**, 135-140.

Kopyscinski, J., Schildhauer, T. J., Biollaz, S. (2010). "Production of Synthetic Natural Gas (SNG) from Coal and Dry Biomass - A Technology Review from 1950 to 2009." *Fuel*, **89**, 1763-1783.

Lunde, P. J., Kester, F. L. (1974). "Carbon Dioxide Methanation on a Ruthenium Catalyst." *Industrial and Engineering Chemistry Process Design and Development*, **13**, 27-33.

Metz, B., Davidson, O., De Coninck, H., Loos, M., & Meyer, L. (2005). *IPCC, 2005: IPCC Special Report on Carbon Dioxide Capture and Storage. Prepared by Working Group III of the Intergovernmental Panel on Climate Change. Cambridge, United Kingdom and New York, NY, USA,* ***442***.

Mignard, D., Pritchard, C. (2008). "On the Use of Electrolytic Hydrogen from Variable Renewable Energies for the Enhanced Conversion of Biomass to Fuels." *Chemical Engineering Research and Design*, **86**, 473-487.

Olivier, J. G. J., Janssens-Maenhout, G., Muntean, M., Peters, A. H. J. (2013). "Trends in Global CO_2 Emissions: 2013 Report." *PBL Netherlands Environmental Assessment Agency*.

Omae, I. (2006). "Aspects of Carbon Dioxide Utilization." *Catalysis Today*, **115**, 33–52.

Pagani, G. (1995). "United States Patent: Process for Urea Production," no. 19: Number: 5,403,956. https://patents.google.com/patent/US5403956A/en.

Pérez-Fortes, M., Bocin-Dumitriu, A., Tzimas, E. (2014). "CO_2 utilization Pathways: Techno-Economic Assessment and Market Opportunities." *Energy Procedia,* **63**, 7968–75.

Pérez-Fortes, M., Schöneberger, J. C., Boulamanti, A., Tzimas, E. (2016). "Methanol Synthesis Using Captured CO2as Raw Material: Techno-Economic and Environmental Assessment." *Applied Energy* **161**, 718–32.

Quadrelli, E. A., Centi, G., Duplan, J. L., Perathoner, S. (2011). "Carbon Dioxide Recycling: Emerging Large-Scale Technologies with Industrial Potential." *ChemSusChem* **4**, 1194–1215.

Quéré, C. L., Moriarty, R., Andrew, R. M., Canadell, J. G., Sitch, S., Korsbakken, J. I., Friedlingstein, P. (2015). "Global Carbon Budget 2015." *Earth System Science Data*, **7**, 349-396.

Rollinson, A. N., Jones, J., Dupont, V., Twigg, M. V. (2011). "Urea as a Hydrogen Carrier: A Perspective on Its Potential for Safe, Sustainable and Long-Term Energy Supply." *Energy and Environmental Science*, **4**, 1216-1224.

Sa, J., Urakawa, A. (2014) "CO_2 to Fuels," in *Fuel Production with Heterogeneous Catalysis*, CRC Press, 93-122.

Sahibzada, M., Metcalfe, I. S., Chadwick, D. (1998). "Methanol Synthesis from $CO/CO_2/H_2$ over $Cu/ZnO/Al_2O_3$ at Differential and Finite Conversions." *Journal of Catalysis*, **174**, 111-118.

Saint Jean, M. D., Baurens, P., Bouallou, C. (2014). "Parametric Study of an Efficient Renewable Power-to-Substitute-Natural-Gas Process Including High-Temperature Steam Electrolysis." *International Journal of Hydrogen Energy*, **39**, 17024-17039.

Schaub et al. (2014). "United States Patent: Process for preparing formic acid by reaction of carbon dioxide with hydrogen," Number: 8,791,297 B2.

Schlereth, D., Hinrichsen, O. (2014). "A Fixed-Bed Reactor Modeling Study on the Methanation of CO2." *Chemical Engineering Research and Design*, **92**, 702-712.

Schmid, J. (2015). *Erneuerbare Energien Und Energieeffizienz Renewable Energies and Energy Efficiency*. *Universität Kassel*, **7**.

Thomas, C., Bonilla, R. J., Huang, Y., Jessop, P. G. (2001). "Hydrogenation of Carbon Dioxide Catalyzed by Ruthenium Trimethylphosphine Complexes Effect of Gas Pressure and Additives on Rate in the Liquid Phase." *Canadian Journal of Chemistry*, **79** (5-6), 719-724.

Van-Dal, É. S., Bouallou, C. (2012). "CO_2 Abatement through a Methanol Production Process." *Chemical Engineering Transactions*, **29**, 463-468.

Websites

www.aspentech.com (last accessed: 20/12/2018)

http://www.eia.gov (last accessed: 20/12/2018)

http://unfccc.int/kyoto_protocol/items/2830.php (last accessed: 20/12/2018)

http://www.cop21.gouv.fr/en/ (last accessed: 20/12/2018)